

Reviewers and Editors,

We have edited our manuscript in response to your feedback. We also made two changes to our manuscript in addition to the changes we made in response to your reviewer comments. We detail these two changes here. We then address your comments in individual responses, appended below. Finally, we have included a version of our manuscript with tracked changes which begins on page 31 of this document.

The additional changes are:

1. We caught a mistake in a calculation in the ikaite discussion. The relevant sentence now reads:

**The ~5 mg ikaite L<sup>-1</sup> sea ice Dieckmann et al. (2008) found in the Antarctic could only enrich  $A_T$  of the surface 100 m by ~1  $\mu\text{mol kg}^{-1}$  for each meter of ice melted, and Arctic surface 100 m  $Alk^*$  is elevated by 59  $\mu\text{mol kg}^{-1}$  relative to the deeper Arctic in our gridded dataset.**

This calculation used to read “~5  $\mu\text{mol kg}^{-1}$  for each meter of ice melted...”

2. We now calculate the gridded dataset volume-weighted mean  $Alk^*$  by ocean basin in Section 3.2 instead of the mean measured  $Alk^*$ . This way we avoid a portion of the measurement distribution bias.

Many thanks,

-Brendan and coauthors

## Response to Reviewer #1

I have embedded specific responses to Reviewer #1's comments below. Reviewer comments are in italicized text and my responses are in plain text. Excerpts from the revised text are in bold.

-Brendan and coauthors

### *Anonymous Referee #1*

*Received and published: 25 July 2014*

*I made two attempts to review this paper but each time became distracted. I was successful on a third attempt -and realized that the length and detail were problematic for me.*

We have shortened the paper and cut back on the level of detail overall, despite adding additional material at the request of reviewers.

*An honest comment is that this reads very much like a thesis with all the style that this implies. It could very well be suitable as a monograph or for a journal that specializes in reviews, but for a mainstream science journal where space and word count are prized it is much too wordy. This is not to minimize the very extensive effort put in to this careful analysis, and there may be room for senior Editorial discretion.*

*I found the insights into the very strong Red Sea signals to be new and interesting (and I would assume that the Persian Gulf might be similar)and that they make great sense. I was less compelled by the extensive riverine input analysis. Those signals are there, and have been known for perhaps a century or so; but seasonal and other*

We retained the Red Sea analysis while cutting back on the analysis of other riverine signals considerably. Other reviewers made similar suggestions.

*temporal changes will occur on a large scale (see Figure 7) and it is likely that individual investigators will make their own adjustments for this on a local basis.*

*Section 4 provides a nice analysis of the influence of competing processes and I found this more useful than the regional analyses that precede it.*

*I think I missed any references to the very high shelf pore water alkalinity and the benthic flux results? I would guess that is more significant than the minor influence of ikaite.*

Pore waters are undoubtedly important reservoirs for  $A_T$  from carbonate dissolution, but we minimize discussion of how they are distinct from other reservoirs for dissolved carbonate minerals because we have little to add to that body of research. We now refer interested readers to a review of this literature (Chen, 2002). Also, we now explicitly include pore waters in "external calcium carbonate cycling:"

**External carbonate cycling refers to input of alkalinity from carbonate minerals dissolved in rivers, hydrothermal vent fluids, sediment pore waters, and submarine groundwater discharge, and carbonate removal by biogenic carbonate burial and authigenic mineralization in sediments.**

*The suggestion of future work (page 18) suggests more of the same. I would have preferred to see some insights into what new experiments, field or laboratory, could be devised or hypotheses tested in some real way.*

We are now provide more detail regarding our suggested future work in the conclusion. Some of which involves forward biogeochemical Earth System Models and is quite different from this study in focus, despite utilizing the  $Alk^*$  tracer.

**We intend to use  $Alk^*$  for two future projects. First,  $Alk^*$  is superior to  $A_T$  for monitoring and modeling changes in marine chemistry resulting from changes in carbonate cycling with ocean acidification.  $A_T$  varies substantially in response to freshwater cycling, so  $Alk^*$  trends may be able to be detected sooner and more confidently attributed to changes in calcium carbonate cycling than trends in  $A_T$ . Preliminary explorations of Earth System Model output suggest time of trend emergence for the alkalinity trends discussed by Ilyina et al. (2009) could be reduced by as much as a factor of 5. Secondly, we will estimate global steady state  $Alk^*$  distributions using  $Alk^*$  sources and sinks from varied biogeochemical ocean circulation models alongside independent water mixing and transport estimates (e.g. Khatiwala et al., 2005; 2007). We will interpret findings in the context of two hypotheses proposed to explain evidence for calcium carbonate dissolution above the aragonite saturation horizon: (1) that organic matter remineralization creates undersaturated microenvironments that promote carbonate dissolution in portions of the water column which are chemically supersaturated in bulk, and (2) that high-magnesium calcite and other impure minerals allow chemical dissolution above the saturation horizon.**

## Response to Reviewer #2

I have embedded specific responses to Reviewer #2's detailed and helpful comments below. Reviewer comments are in italicized text and my responses are in plain text. Excerpts from the revised text are in bold.

-Brendan and coauthors

### Reviewer 2:

*Carter et al. introduce a new composite tracer Alk\* in order to 'isolate the impact of acidification on biological calcification and remineralization' (abstract). Total alkalinity (AT) in the ocean changes due to several processes: (1) evaporation/precipitation, (2) formation of organic matter by phytoplankton, (3) remineralization of organic matter, (4) formation/dissolution of CaCO<sub>3</sub>, (5) redox processes in marine sediments and in the water column, (6) riverine input of water with varying alkalinity (usually, however, not always smaller than mean seawater concentrations). Carter et al. are especially interested in (4) formation/dissolution of CaCO<sub>3</sub>, which is difficult to quantify for the world oceans. They propose a new tracer (Alk\*) that should ideally be a tracer of CaCO<sub>3</sub> cycling alone.*

*The definition of Alk\* is a bit more tricky than for other \*-quantities:*

$$\text{Alk}^* = \text{AT} + 1.26 * [\text{NO}_3^-] - S * \text{mean}(\text{AT} + 1.26 * [\text{NO}_3^-]) / \text{mean}(S) \{\text{Alk}^*\text{def}\}$$

*where the mean values are calculated over the 'top 50 meters of the ocean' (actually averaged vertically as well as horizontally yielding a value of 66.4 mol kg<sup>-1</sup> for mean(AT + 1.26 \* [NO<sub>3</sub><sup>-</sup>]) / mean(S), compare Eq. 5), AT is the total (or titration) alkalinity and S is the salinity. The term 1.26 times the nitrate concentration takes care of AT changes due to formation of organic matter by phytoplankton (uptake of nitrate, phosphate, sulphate) or the remineralization of organic matter. The value of the coefficient can be either taken from observations (1.26 based on Kanamori and Ikegami, 1982) or derived from the stoichiometry (N:P:S; Redfield & extensions; for details compare Wolf-Gladrow, D. A., Zeebe, R. E., Klaas, C., Körtzinger, A., and Dickson, A. G.: Total alkalinity: the explicit conservative expression and its application to biogeochemical processes, Marine Chem., 106, 287–300, 2007.) of phytoplankton.*

*The sum of the first two terms on the rhs of {Alk\*def} is called 'potential alkalinity' Ap: Ap = AT + 1.26 \* [NO<sub>3</sub><sup>-</sup>]*

*Ap is a conservative quantity with respect to organic matter production based on nitrate uptake (decrease of nitrate & increase of AT) and remineralization of organic matter (inclusively oxidation of reactive nitrogen to nitrate).*

*Please note that Alk\* can take on positive as well as negative values. The surface ocean mean (upper 50 m) of Alk\* is zero by definition. The depth of 50 m used for the definition of Alk\* is rather arbitrary and in my opinion a weakness of the proposed Alk\* concept.*

This is a fair and concise summary of the tracer.

*The discussion on regional variations of AT and Alk\* and the influence of riverine alkalinity input is quite insightful. Another interesting region with 'unusual' alkalinity values is the Mediterranean Sea (compare, for example, Schneider, Anke, Douglas WR Wallace, and Arne Körtzinger. "Alkalinity of the Mediterranean Sea." *Geophysical Research Letters* 34.15, 2007).*

Also true, we did little with this because we had little to add to it.

*I found it difficult to grasp the content of the section on process importance on saturation level (I had to read it several times). The case of atmospherically isolated water masses applies mainly to deeper layers (below the surface mixed layer, below the euphotic zone) and thus I suggest to use the terms remineralization of organic matter (instead of organic matter cycling) and carbonate dissolution (instead of carbonate cycling). The results are given in Table 1: the globally most important processes for changes in are cycling of (1) organic matter and (2) carbonate and (3) pressure changes (not really surprising) whereas temperature changes are of minor importance.*

This is a good point. However, other reviewers have noted that our “atmospherically isolated seawater” case applies also to surface seawater on short timescales. We therefore feel the more general terms (including organic matter formation and calcium carbonate precipitation) are more appropriate.

*When the water sample has the change to equilibrate with the atmosphere (i.e. in the surface ocean), production of organic material has a smaller impact on mainly via the associated change of AT by nitrate uptake. Freshwater cycling has a large input on AT and (for the Arctic Ocean compare, for example, Yamamoto-Kawai, Michiyo, et al. "Aragonite undersaturation in the Arctic Ocean: effects of ocean acidification and sea ice melt." *Science* 326.5956 (2009): 1098-1100.). I don't understand why you discuss pressure changes in this context (surface ocean!),*

Pressure changes (and the influence of pressure changes on calcite saturation) are indeed minimal in the surface ocean. We thought about not presenting these  $M$  and  $I$  values, though we feel it requires very little additional language/space to include it. Also, including this discussion will allow people concerned with the controls on calcium carbonate saturation in the euphotic zone to confidently ignore the pressure differences between the surface and whatever depth surface the calcifying organisms are found at. Finally, removing this term begs the reader to ask how we can compare  $I$  values for well-equilibrated waters to  $I$  values determined for atmospherically isolated seawater when we are dividing by the sum of a different number of  $M$  values.

*Process importance (Appendix A): I found it difficult to read Appendix A. If I understand it right the authors calculate the propagation of standard deviations for single processes similar to the standard method known as 'combination of errors' where products of variances and squared partial derivatives are added for various independent variables.*

This is not quite accurate.

*The problem here is the complicated dependency of the saturation level on various quantities and processes. In a single process various quantities can co-vary and impact via different 'routes'. The authors try to take these complications into account by summing over seven products of partial derivatives (Eqs. A3 and A5; products stemming from chain rule). In total five different equations are given for the metric  $M_i$ . Finally, the authors apply Monte Carlo simulations to estimate variability and uncertainty of the metric (which of the five versions given?).*

We decided that additional clarity was required. We have reduced the number of equations for  $M$ , and now explicitly state which equation is used to calculate  $M$ .

The comment about the different 'routes' is certainly also correct. This was the motivation for our Monte Carlo analysis where we allowed the initial state of the seawater to vary to reflect the range of possible seawater states and compositions that would result through the action of the processes we consider. As noted, we found that the impact of a process varied strongly with the initial state and composition of the water considered. However, the impact of the processes relative to other processes did not. This distinction is why we present different uncertainties/variabilities for our  $M$  and  $I$  metrics.

*Throughout the manuscript, the authors talk about 'carbonate cycling' and it remains ambiguous whether they refer to carbonate ions ( $\text{CO}_3^{2-}$ ) or calcium carbonate minerals ( $\text{CaCO}_3$ ). Also 'carbonate saturation': replace by carbonate saturation state, introduce which is used later on and give equation.*

We followed this recommendation.

**Further points:**

*The authors fail to give a thorough introduction into the topic.*

We reorganized our background material in light of this and the following comments.

*p. 11140, L. 20: The tracer  $\text{Alk}^*$  should not be introduced in the introduction, but in the next section "The tracer  $\text{Alk}^*$ ".*

We now only mention  $\text{Alk}^*$  at the end of the introduction (formerly it was at the start), in the paragraph in which we give an overview of the paper.

*11140, L. 20:*

*... to isolate the influences carbonate cycling ... ->*

*... to isolate the **influence of** carbonate cycling ...*

Changed

*p.11141, L. 20: operational definition gives AT ->*

operational definition gives  $A_T$  (measured in  $\text{mol kg}^{-1}$ , gravimetric units)

We now state “ $A_T$  (expressed in  $\text{mol kg}^{-1}$ )”

*p. 11141, L. 6-8: This is summary and outlook and is misplaced in the introduction. A proper introduction could include an introduction to the carbonate system, calcium carbonate minerals, the concept of alkalinity (parts of section 2 could go here), sources of alkalinity (parts of section 3 could go here, p. 11145, lines 8-17) including the role of rivers, and then at the end the main questions posed for this paper.*

We now indicate that rivers are a major alkalinity source in the introduction.

*p.1142 L. 5-6:*

*... while still mixing and responding to calcium carbonate cycling linearly. ->*

*... while still mixing **linearly** and responding to calcium carbonate cycling.*

Changed.

*p. 11142, L. 17-19: This sentence is unclear. What is the link between export of organic matter and release of  $\text{OH}^-$ ? Also, you say a ‘1:1 release of proton acceptors’ - this is a ratio, so 1:1 release per what?.*

*I assume you refer to an increase of alkalinity by 1 mole when 1 mole of N from nitrate or nitrite is assimilated (Wolf-Gladrow et al., 2007), but please take the time to make the explicit link (from export) to nitrate.*

We clarified this statement:

**Nitrate uptake for anaerobic denitrification and the production of amino acids occurs in an ~1:1 mole ratio with the release of molecules that increase  $A_T$  (Chen 2002).**

*p. 11143, L. 1-5, you're too fast: switch sentences, first introduce empirical value by Kanamori and Ikegami, give equation, then the sentence with the comparison to theoretical value by Wolf-Gladrow et al (give number here, too).*

We followed this recommendation:

**We thus use the ratio found by Kanamori and Ikegami (1982) to define potential alkalinity ( $A_p$ ).**

$$A_p = A_T + 1.26 * [\text{NO}_3^-] \quad (1)$$

**While the empirical ratio of 1.26 may be specific to the elemental ratios of the North Pacific, Wolf-Gladrow et al. (2007) provide a theoretical derivation from Redfield ratios and obtain a similar value of 1.36.**

*p. 11143, salinity normalization of Robbins (2001). This is a very important part of your Alk\* calculation and therefore needs some more explanation besides referring to Robbins. Go step by step, don't mention the subtraction in line 14 yet, that is not relevant here for the definition of what you call 'passive conservative potential alkalinity'. Also give the number for averaged Ap (line 19/20).*

We also followed this recommendation.

*p. 11143, L. 20: this is a typical sentence that was written without due diligence: "The mean surface values are chosen to capture the impact of freshwater cycling where precipitation and evaporation occur." After reading the sentence three times, I realized it should read: "The mean surface values were chosen because \*we assume that they\* capture the impact of freshwater cycling where precipitation and evaporation occur." Sentences like this one are manifold throughout the manuscript.*

We mostly followed this recommendation:

**The mean surface values are chosen in an effort to best capture the impact of freshwater cycling where precipitation and evaporation occur.**

This phrasing seems preferable to suggesting that we assume our approach captures this influence perfectly, which we do not. Instead, we aim to do the best we can with a single value.

*p. 11144, after eq. 5 add eq. 6 where you give the full equation:  $Alk^* = AT + 1.26 NO_3^- - 66.4 S$ . Don't add the unit in eq.5 but give it below as: "where Alk\* has same units as AT ( $\mu\text{mol kg}$ )."*

Done.

*p.11144 L.8: Mean global surface Alk\* is zero by definition, and negative Alk\* is possible when potential alkalinity is less than expected from salinity. ->*

*Mean global surface Alk\* is zero by definition, and thus Alk\* can take on positive as well as negative values.*

Done (we switched "negative" and "positive" in R2's recommendation since we think negative will be more alarming to first time readers).

*p. 11144, l. 14-23: this paragraph comes as a surprise, it is unclear why this is discussed here. This is because the Robbins paper was not thoroughly introduced (see comment above). Maybe it should be in an extra paragraph or section "Evaluation of the tracer Alk\*". It definitely needs more explanation of why this is important.*

Due to this and other reviewer comments, we moved this discussion to supplementary materials (see other response to reviewers).

*p. 11145, l. 1-17: AT and Alk\* seem to be used intermittently. Do you want to talk about AT or about Alk\*. The part of introducing sources for AT should be moved to the introduction.*

We followed this recommendation.

*Line 14-17: this is disconnected to the previous paragraph, convert to alkalinity units.*

Done.

*p.11146 L.2: The Alk\* distribution has a broadly similar explanation to the phosphate distribution. MAY NEED MORE EXPLANATION*

We rewrote this section, and this sentence is now missing (see responses to R4 for more).

*p. 11146 L.6: Several qualitative differences between Alk\* and phosphate are visible in Figs. 2, 4, and 5. ->*

*Several differences between Alk\* and phosphate patterns are visible in Figs. 2, 4, and 5.*

Added “distributions” in place of patterns for consistency with our terminology in the rest of the manuscript.

*p.11146 L.10: a maxima -> a maximum*

Changed

*p.11147, L1: The nearly-zero mean surface Pacific Alk\* indicates that Alk\* supply from upwelling and a small riverine source very nearly balances carbonate precipitation. THE FACT THAT THE MEAN SURFACE ALK\* OF THE PACIFIC MIGHT IN PART BE DUE TO THE LARGE SURFACE AREA AND THE BY DEFINITION ZERO GLOBAL MEAN OF SURFACE ALK\*.*

We removed this sentence.

*p.11148, L.21: I suggest to drop ‘The higher Alk\* found for May through July is consistent with Moore et al. (1986)’s radium isotope based finding that 20–34% of the surface waters in this region are derived from Amazon during July vs. 5–9% during December. However, if we assume the Atlantic seawater mixing with the Amazon outflow had an Alk\* of 25–35  $\mu\text{mol kg}^{-1}$ , these Amazon River water fractions would result in Alk\* of  $-15$  to  $0 \mu\text{mol kg}^{-1}$  in December and 45 to  $100 \mu\text{mol kg}^{-1}$  in July. We see lower Alk\* values in our distribution and a smaller disparity between winter and summer Alk\*, suggesting a smaller average Amazon influence for the ocean’s surface during both seasons than found by Moore et al. (1986). However, our estimate does not account for any changes in calcium carbonate export induced by nutrient-rich Amazon outflow.’ because it leads to nowhere.*

We dropped everything after an altered version of the first sentence (see responses to R3).

*p. 11149, l. 4: "intermediate to high": give numbers*

This paragraph was removed.

*p. 11150, L.3: This bay has two high AT rivers that join and flow into it, the Brahmaputra (1114 mol kg<sup>-1</sup>) and the Ganges (1966 mol kg<sup>-1</sup>) (Cai et al., 2008).*

->

*This bay has two high AT rivers that join and flow into it, the Brahmaputra (AT = 1114 mol kg<sup>-1</sup>) and the Ganges (AT = 1966 mol kg<sup>-1</sup>) (Cai et al., 2008).*

*or (???)*

*This bay has two high AT rivers that join and flow into it, the Brahmaputra (Alk\* = 1114 mol kg<sup>-1</sup>) and the Ganges (Alk\* = 1966 mol kg<sup>-1</sup>) (Cai et al., 2008).*

This paragraph was removed.

*Section 3.3: Riverine Alk\* regionally: what information is added by this discussion to the study of Cai et al (2008) on alkalinity contribution from rivers? Why is Alk\* needed for that discussion?*

We removed most of this, but we still think Alk\* is useful for discussing the (smaller than expected) role of the Amazon, and the (larger than expected) Red Sea Alk\* deficit.

*p. 11153, l. 7-8: what is the outcome of testing this assumption?*

We expanded on this discussion:

**We test the validity of this assumption by also estimating  $M$  for the observed global  $p\text{CO}_2$  variability in the Takahashi et al. (2009) global data product. This test reveals transient air-sea disequilibria are indeed important for surface ocean calcite saturation, but only as a secondary factor when considered globally. Despite this, it is important to recognize that air-sea equilibration following a process is not instantaneous, and that the  $S_{R_i}$  value estimates in section 4.1 will be better for estimating short term changes following fast acting processes such as spring blooms (e.g. Tynan et al., 2014) or upwelling events (e.g. Feely et al. 1988).**

*p. 11154, l. 2-6: it would be more informative to plot temperature versus surface calcite saturation in a x,y-plot or at least calculate a correlation and give that number.*

Added a correlation coefficient.

*section 5: Conclusions: not all that is written here is a conclusion by definition, e.g: p. 11154, L. 17-18: "A plot of Alk\* against salinity reveals the large AT input from the Amazon River". That is a sentence for the results section. The conclusion section should be considerably shortened and be reduced to main conclusions. It should include a paragraph on: what are advantages of the Alk\* method, why is it needed, what can we use it for that cannot be achieved by AT alone?*

We truncated this section considerably.

*Figures:*

*The choice of figures seems arbitrary. They are randomly introduced but not discussed at the same time. Page 11145, L. 19-21: First sentence introduces Figure 2. Second sentence introduces Figure 3. There is no discussion of Figure 2.*

We have rewritten our text to better explain why we chose the figures we did, and to better guide the reader from figure to figure (see below for text).

*What is the added value of showing the top 50 m mean right after showing the surface values? I can't see any.*

We now explain why we have Figure 1 (was Fig. 2):

**Figure 1 maps surface  $Alk^*$  (top 50 m) at the measurement stations. We provide this figure to show where we have viable  $Alk^*$  estimates and to demonstrate that our gridded data product adequately captures the measured  $Alk^*$  distribution. Figure 2 maps gridded global surface  $A_T$ , salinity,  $Alk^*$ , and phosphate distributions and mask the regions that are lacking data in Fig. 1.**

*In line 26 it becomes even clearer: "The subtropical gyres have the lowest open ocean  $Alk^*$  in Figs. 2, 3 and 4." First, this is badly formulated, but then if you can see the same thing in three figures, two of them are not needed, right?*

We rewrote this section generally to make it more clear how we are using each figure:

**The similarity of the  $A_T$  (Fig. 2a) and salinity (Fig. 2b) distributions demonstrates the strong influence of freshwater cycling on the surface marine  $A_T$  distribution (see also: Millero et al. 1998, Jiang et al., 2014). The dissimilarity between  $Alk^*$  (Fig. 2c) and salinity (Fig. 2b) suggests  $Alk^*$  removes the majority of this influence. The phosphate (Fig. 2d) and  $Alk^*$  (Fig. 2c) distributions are similar at the surface. They are also similar at depth. Figures 3 and 4 show zonally-averaged gridded depth sections of  $Alk^*$  and phosphate.  $Alk^*$  and phosphate concentrations are low in the deep Arctic Ocean (Figs. 3d, and 4d), intermediate in the deep Atlantic Ocean (Figs. 3a and 4a), and high in the deep North Pacific (Figs. 3b and 4b) and deep North Indian (Figs. 3c and 4c) Oceans.  $Alk^*$  and phosphate distributions are similar because similar processes shape them: the hard and soft tissue pumps transport  $A_T$  and phosphate from the surface to depth, respectively. The "oldest" water therefore has the highest net phosphate and  $Alk^*$  accumulation. High surface phosphate and  $Alk^*$  in the Southern Ocean and North Pacific in Figs. 2, 3, and 4 are due to upwelled old deep waters.**

**Several qualitative differences between  $Alk^*$  and phosphate distributions are visible in Figs. 2c, 2d, 3, and 4. Surface phosphate is low in the Bay of Bengal and high in the Arabian Sea (Fig. 2d), while the opposite is true for  $Alk^*$  (Fig. 2c). Also,  $Alk^*$  reaches its highest surface concentration in the Arctic (Figs. 2c and 3d) where phosphate is not greatly elevated (Figs. 2d and 4d). These surface differences are due to regional riverine  $Alk^*$**

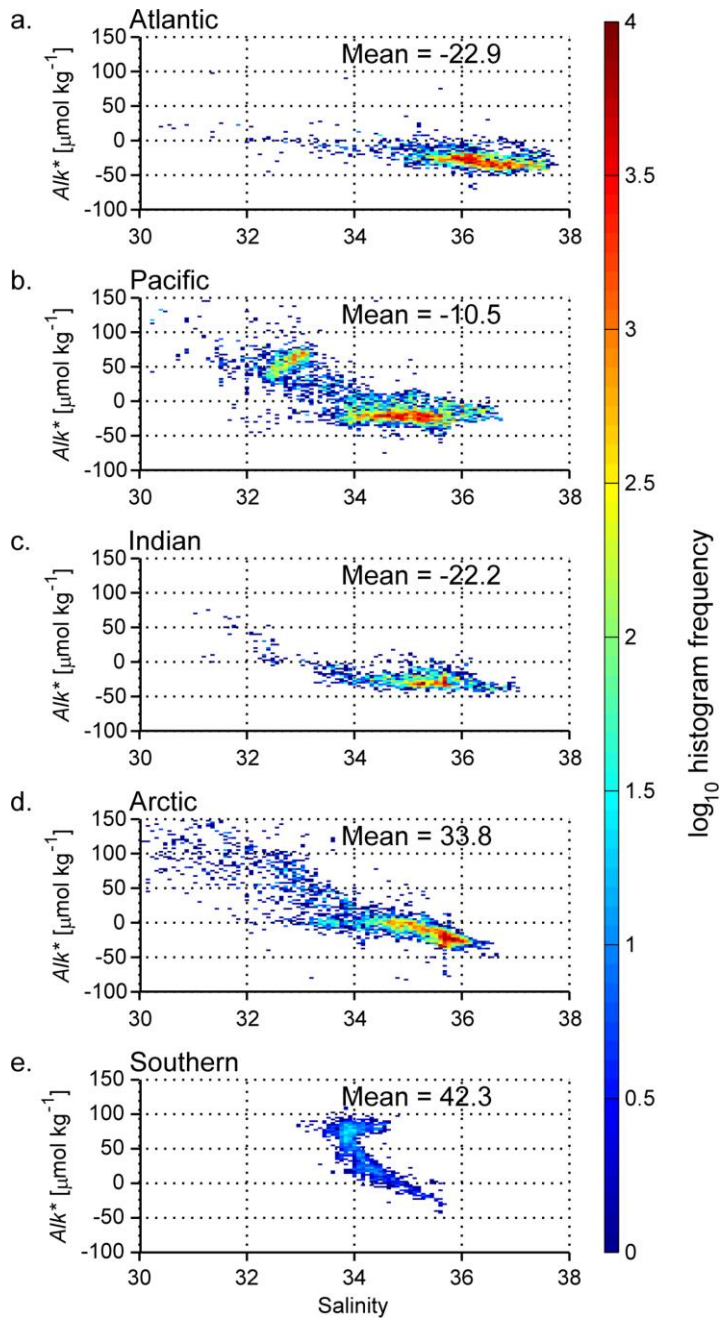
inputs (Section 3.3). Another difference is that  $Alk^*$  reaches a maximum below 2000 m in all ocean basins except the Arctic, while phosphate maxima are above 2000 m. We attribute the deeper  $Alk^*$  maxima to deeper dissolution of calcium carbonates than organic matter remineralization. Finally,  $Alk^*$  values are higher in the deep Indian Ocean than in the deep Pacific. This is likely due to elevated biogenic carbonate export along the coast of Africa and in the Arabian Sea (Sarmiento et al., 2002; Honjo et al., 2008).

*I suggest to: introduce one figure. Then discuss it. Then introduce the next figure. Then discuss it. Take out the figures where there is no extra information to be discussed.*

We followed this suggestion in the text above.

*Same in Figure 6, p. 11146, line 18: In the "2D color histograms" the colors and number of data points for certain bins are not further discussed, so the graph could be more simple without colors.*

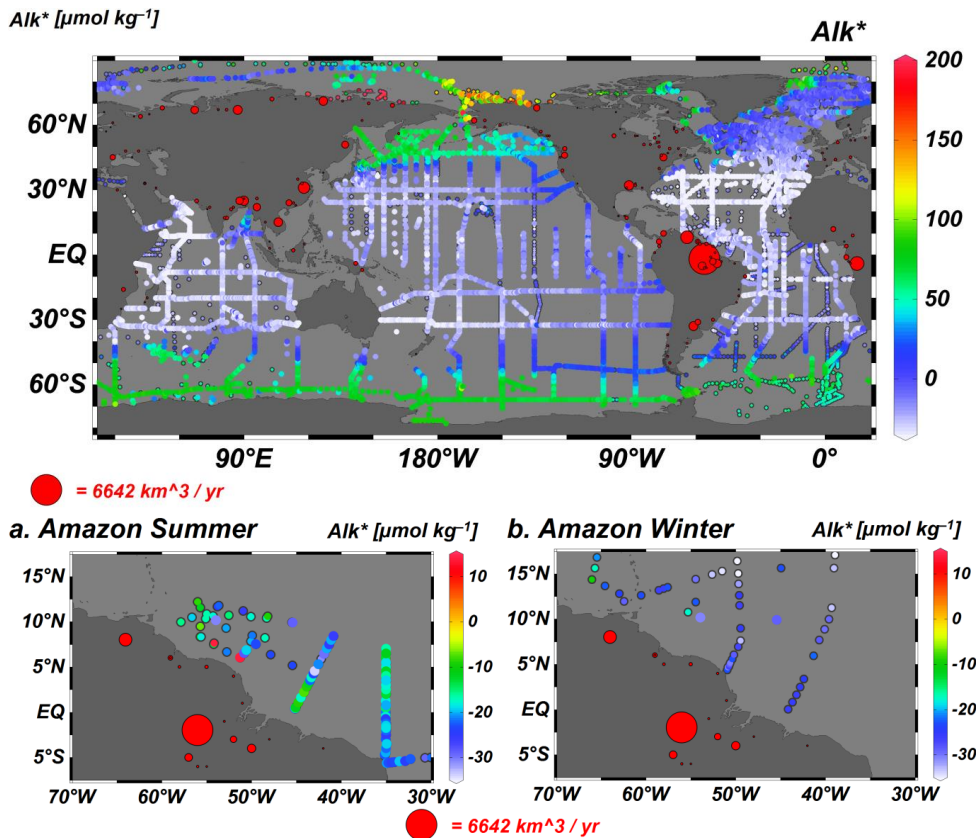
We feel it important to note that the majority of the data fall within specific bins. For example, without the color histogram, the rare measurements near river mouths in the Arctic would have nearly the same visual impact as the elevated North Pacific  $Alk^*$ . We did remove un-discussed detail by eliminating an entire panel of  $A_T$  vs.  $S$  histograms, however:



All figures need a revision, just some examples:

\* Figure 3: legend for size of dots missing

We have added a legend to this figure and Figure 6 (was Figure 7).



\* Figure 4: the figures look like prepared with ODV. One very helpful feature of ODV is that one can have dots to indicate where samples were taken. This illustrates the density of measurements and gives a feeling of how much one can trust the interpolation. This should be applied here.

This figure is a zonal average plot of gridded data. Showing where our gridded data was located would just be revealing what we chose for our grid. As a zonal average, showing all measurements within a given basin (measurements we used to determine our gridded data) would both clutter the figure with a tremendous number of dots and mislead the reader into assigning the wrong weights to isolated points. For instance, a measurement that appears in the middle of a clump of other measurements may actually have a large influence on the plot if it is separated from other points longitudinally.

*\* Figure 7: Dots for river outflow are plotted on land.*

With the exception of one suspected typo (an Alaskan river in the central Pacific) we had no choice but to plot these points where Dai and Trenberth located them. If we moved them, we'd be guessing at the true river mouths, and, I believe, we'd be indicating the incorrect location at which the flow is estimated.

*p. 11156 Eq. (A2) one '∂' missing in eq.*

Fixed.

*p.11166/7 Tables A1 & A2: Units missing for the partial derivatives (some are dimensionless, however, others possess units).*

Fixed.

### Response to Reviewer #3

I have embedded specific responses to Reviewer #3's detailed and helpful comments below. Reviewer comments are in italicized text and my responses are in plain text. Excerpts from the revised text are in bold.

-Brendan and coauthors

#### *Anonymous Referee #3*

*Received and published: 15 September 2014*

*Review of "Processes determining the marine alkalinity and carbonate mineral saturation distributions" by Carter et al.*

*This paper presents some interesting analysis of alkalinity and carbonate saturation. The analysis and main conclusions are on the whole (although not always) reasonable and well-founded. Some aspects of the analysis can benefit from improvement. The manuscript is generally clear and fairly well written but some sections need attention and previous work is often not acknowledged.*

*Overall recommendation: resubmit following revision*

*Main comments:*

*1-3, 98: The way the text is written makes it seem as if it is a benefit to have a composite tracer, one that also "highlights" river alkalinity plumes. However, the general philosophy of developing tracers is normally to subtract off as many confounding influences as possible so as to get to a variable that (ideally) traces the activity of just one biogeochemical process, or if not just one then as few as possible. The more competing influences (multiple processes) that impact on a tracer, the harder it is to deconvolve them in order to use the tracer to assess the rate of just one, and in general the less useful the tracer is. For the topic of this paper, it is less useful to have a tracer that is influenced by both carbonate cycling at sea and carbonate cycling on land (via rivers), because variation in the tracer cannot then be attributed unambiguously to either one or the other. This can be seen in, for instance, in lines 210-214. On line 3 the word "highlights" should be replaced with something more appropriate (e.g. "is also affected by"); likewise "preserves" should be changed to "is altered by" or similar wording on line 98.*

We made the recommended changes (by replacing "highlights" with "is also affected by" and eliminating the portion of the sentence in which "preserves" appears. We think it is important to emphasize that  $Alk^*$  retains riverine alkalinity because earlier readers missed that point and became confused later.

*52-61: there are a number of problems with the nitrogen cycle section. The chemical processes are all unidirectional rather than reversible and hence one-way arrows should be used.*

*Ammonia (NH<sub>3</sub>) should be replaced by ammonium (NH<sub>4</sub>) because this is the dominant form (~90%) at typical seawater pH. Nitrification converts ammonium to nitrite to nitrate (in two steps); not the opposite reaction as stated in R1. Nitrogen fixation initially creates PON from N<sub>2</sub>. It is only later following the creation of ammonium from PON (ammonification) during nitrogen fixer decay and after that nitrification to convert the ammonium to nitrate that nitrate is eventually produced.*

We originally tried to combine several reaction pathways for brevity. In this draft we decided to limit this discussion further and provide the following summary sentences, which address only the material we need to make clear:

**Nitrate uptake for anaerobic denitrification and the production of amino acids occurs in an ~1:1 mole ratio with the release of molecules that increase  $A_T$  (Chen 2002). Similarly, nitrate produced by fixation of nitrogen gas and remineralization of amino nitrogen is released in a 1:1 mole ratio with acids that titrate away  $A_T$  (Wolf-Gladrow et al., 2007).**

*Section 3.3: This section is a little weak and not as tightly written as most of the rest of the MS. The tracer is less useful for quantification in heavily river-influenced areas because of the dual influences of in-situ calcification/dissolution and river effects, with uncertainty about how to separate the two. This section could perhaps be streamlined to include only rivers impacting on the open ocean. It would certainly help the reader follow the logic if some explanation could be given as to why Alk\* is calculated for rivers such as the Daugava which empties into the Baltic Sea, and the Yangtze which empties into the Yellow Sea, both of which places are blacked out (because no carbonate system data) in figure 2c.*

We cut a lot of material here, including everything having to do with the marginal seas and about half of what we had devoted to the Amazon. We did this for brevity and because this section doesn't add much, as Reviewer 3 and others pointed out.

*Section 4: There is a fairly abundant although scattered literature of prior work on this topic, at least some of which should be cited. The results developed here need to be critically compared to findings from other work (for instance Orr et al 2005), including regional observational studies, for instance Yamamoto-Kawai et al 2009, Bates et al 2009, Mathis et al 2012, Shaw & McNeil 2014, Tynan et al 2014. While the results obtained from deep water seem to be broadly consistent with previous work, those from surface water are less so. In particular, the inferred importance of organic matter cycling seems very low in comparison to other work (Tynan et al 2014 in particular).*

We have endeavored to add mention of some of these papers (see text below, starting with “**Despite this...**”)

However, I'm not convinced that these papers are directly comparable to our discussion. The cited studies address the controls on variability at a given location over time. By contrast, we focus on why various regions throughout the world have such different baseline carbonate saturations about which they vary with time. Analogous seemingly-contradictory (but not mutually exclusive) findings would be: “Arizona has some big storms” and “Arizona is an arid place relative to the rest of the world.”

*This is probably due to the problematic assumption in this study that surface seawater is in equilibrium with an atmosphere of 400 ppmv CO<sub>2</sub>, although the authors also calculate without this assumption. While the assumption of air-sea equilibrium is reasonable over broad swathes of the (relatively quiescent) tropical and subtropical oceans, it is often strongly violated at high latitudes, with large and long-lasting depressions in pCO<sub>2</sub> (e.g. >100ppmv) caused by spring phytoplankton blooms. Either the analysis should be revised to more fully explore and take account of this flawed assumption, or else the reason for the discrepancy between the findings here and in other studies should be more fully explained. The authors are doubtless correct about the strong importance of temperature, although it is not clear that the reason for the importance of temperature is understood. The underlying reason is the effect of temperature on gas solubilities (CO<sub>2</sub> solubility) and hence CO<sub>2</sub> gas exchange (see in particular figure 6.5 and chapter 6 of Williams and Follows 2011).*

In our defense, we made this link explicitly in the abstract in the previous version... though we perhaps make it more clearly now:

**We show regional differences in surface calcite saturation are due to the effect of temperature differences on CO<sub>2</sub> solubility and, to a lesser extent, differences in freshwater content and air-sea disequilibria.**

*Larger inputs of deep water to high latitude surface water may also be important (Orr et al., 2005). These should be mentioned. Again previous work on the topic should be acknowledged and the findings of this study related to (and explained in the context of) previous findings.*

Regarding Tynan et al. 2014, they have a nearly opposite finding to our own... specifically they find organic matter formation is important and the effects of temperature changes are negligible. However, this is because their calculations presume that all saturation change from organic matter formation occurs without the opportunity for re-equilibration. Similarly, they do not account for the changes in equilibrium  $C_T$  with changes in temperature. They therefore essentially use a calculation equivalent to our poorly-equilibrated-seawater calculation. Casual inspection of their data suggests that the temporal variability in carbonate saturation could be reasonably well explained by temperature variability if they allowed for the influence of temperature on equilibrium  $C_T$ . I do not mean to imply they are wrong, merely that presuming no gas exchange is just as perilous as presuming complete gas exchange. We try to presume neither. Instead, we try to make it clear here that our two calculations represent extreme cases and that the appropriate calculation will depend on the timescale considered. We've added the following text to highlight this distinction:

**Despite this, it is important to recognize that air-sea equilibration following a process is not instantaneous, and that the  $S_R$  value estimates in section 4.1 will be better for estimating short term changes following fast acting processes such as spring blooms (e.g. Tynan et al., 2014) or upwelling events (e.g. Feely et al., 1988).**

*Appendix A: this is very hard to follow. The analysis is over-elaborate and could probably be simplified without loss of rigour. It is not clear why so many steps are required for what is seemingly quite a simple calculation. Example calculations should be shown to make the explanations more concrete.*

We have tried to simplify this further several times. We tried again with this draft (see our response to Reviewer 2), but most more invasive options that we came up with do require some loss of rigor. We did add an example calculation as appendix SE, however.

*Detailed comments:*

6-7: according to Fig 2c, net carbonate precipitation lowers  $Alk^*$  across the low latitudes in all basins, not just the Indian and Atlantic.

We were originally referring to the mean values, which by themselves do not support this correct statement (due to upwelling in the North Pacific). We still emphasize the Indian and the Atlantic in the Abstract because these two oceans had lower mean  $Alk^*$ , even when only considering the subtropics. We rewrote portions of the basin mean value discussions to make this clear, and changed this portion of the abstract to read:

**Strong net carbonate precipitation results in low  $Alk^*$  in subtropical gyres, especially in the Indian and Atlantic Oceans.**

24: why work with gridded rather than bottle data? A reason should be given.

We now give our reason:

**We use our gridded dataset to limit sampling biases and to enable us to make volume-weighted mean property estimates.**

72: potential alkalinity usually also includes salinity normalisation. The definition here is unusual.

The original potential alkalinity from Brewer et al. 1975 did not normalize to salinity, though Reviewer 3 is correct that there have been papers that refer to it as though it did.

106-107, fig 1: Jiang et al 2014 discusses the non-linearity of NTA and the consequence thereof. It is done in greater detail and with greater rigour, and can be cited for this point. Fig 1 could be deleted.

This very recent paper did help simplify the discussion of this topic. We now refer to Jiang et al. (2014) in the discussion, and we have moved most of our calculations to supplementary materials.

**In Supplementary Materials document SC we demonstrate that  $Alk^*$  mixes conservatively, and briefly contrast  $Alk^*$  to traditionally normalized potential alkalinity which does not mix conservatively (Jiang et al., 2014).**

137: is the physical process always upwelling?

If I understand the question correctly, then I believe yes.

154: presumably "Net precipitation in the tropics and net evaporation in the subtropics..."

Correct. We changed the text in this draft to read as presumed.

*180-187: which of these differences are statistically significant?*

This is a tough question to answer well, and an even harder one to answer in few words. Uncertainty on the gridded  $Alk^*$  values can be estimated from the differences between measurements and the gridded values at each measured location. However, this is likely an uncertainty overestimate because measurements and the gridded data can disagree without either being wrong... simply because they represent different quantities (one is averaged in time and space and the other is not). Nevertheless, using this approach suggests our gridded estimates have a standard uncertainty of  $\sim 10 \mu\text{mol kg}^{-1}$ . When we consider that we are averaging a large number of these gridded values (6092 for the Atlantic) the uncertainty on the mean value becomes quite small ( $\sim 0.1$ ) if we presume (almost certainly incorrectly) that the errors in the gridded values are uncorrelated. Given the many caveats to this assessment, I am not confident saying that the Atlantic and the Indian have different mean  $Alk^*$  values. I am confident that all other oceans are different, as defined, however. This thinking motivates the language we use to frame this discussion.

*182:  $Alk^*$  cannot be measured directly. This should be reworded, for instance: "The Atlantic has the highest measured TA in the open-ocean surface but the lowest  $Alk^*$  and..."*

Good point. We removed the word "measured" here and elsewhere.

*185-187: A near-zero mean value does not imply balance. All basins must be balanced unless the authors are making the unlikely suggestion that mean values are changing over time where  $Alk^*$  is high.*

We clarified our meaning in this version:

**Considering the weak Pacific riverine input, this suggests that, relative to other ocean basins, there are either larger  $Alk^*$  inputs from exchange with other basins and deeper waters or smaller Pacific basin mean net calcium carbonate.**

*203-214, 354-355: This section should be deleted (along with figure 7?) unless anything new can be said compared to the papers by Cooley et al (2006; 2007), which should be cited. The conclusion is not new.*

We truncated this section and cited the Cooley et al. (2007) paper.

**However, the influence of the Amazon on  $Alk^*$  can be seen in the seasonal  $Alk^*$  cycle in the Amazon plume. Figure 7 provides a map of  $Alk^*$  for this region scaled to show the influence of this low  $Alk^*$  river in the Northern Hemisphere (a) winter and (b) summer months. The higher  $Alk^*$  found for summer months is consistent with Amazon discharge and  $A_T$  seasonality (Cooley et al., 2007) and Moore et al.'s (1986) radium isotope based finding that Amazon River outflow comprises 20-34% of surface water in this region in July compared to only 5-9% in December.**

251: Jiang et al 2014 should be cited for low alkalinity values in the Red Sea, and calcification as the reason. They carry out a more thorough separation of salinity and calcification effects, reaching the same conclusion. It could be noted that the analysis is stronger for Red Sea than for elsewhere because no sizeable rivers flow into the Red Sea and so decreases in Alk" can be attributed straightforwardly to calcification.

We tried to keep out discussion brief:

**Like Jiang et al. (2014), we attribute low Red Sea Alk\* to exceptionally active calcium carbonate formation.**

268: better in what way?

We have clarified that we are referring to the fact that the magnitude of the feature could not be explained by ikaite cycling.

**However, riverine  $A_T$  inputs better explain the magnitude of the feature:**

280-281: delete "are". Reword "depth changes of seawater".

We changed this to "pressure changes of seawater" for clarity.

337: salinity is not normally expressed in units of g/kg.

Fixed

339: the sentence should be reworded to explain that it is not the current (deep) temperature that ensures high 52, but rather the warm temperature when it last left the surface (which would have ensured CO<sub>2</sub> outgassing until the surface seawater was driven to a low [CO<sub>2</sub>(aq)] commensurate with a CO<sub>2</sub> partial pressure of ~400 ppm at low solubility; when low CO<sub>2</sub> concentration is achieved through gas exchange then it drives carbonate ion concentration to high values).

We struggled with how to (and whether to) clarify our meaning here in the last draft as well. In this draft we say:

**The deep Red Sea is also unusual for having deep water that was warm when it last left contact with the atmosphere (the Red Sea is >20 °C at >1000 m depth). This provides high initial deep calcite saturation that—combined with decreased influence of pressure changes at higher temperatures—keeps deep Red Sea  $\Omega_C > 3$ .**

362-364: temperature has little direct effect on 52 (table 1.1.6 of Zeebe & Wolf-Gladrow 2001) so it is confusing to include both temperature and air-sea gas exchange in this sentence. A high rate of primary production (to be expected in river plumes) is a more common way of inducing a strong increase in 52.

We got rid of this sentence during our pruning of the conclusions section.

*367-368: calcium carbonate cycling is also usually less important to S2 than organic matter cycling, even in coral reef lagoons.*

Interesting!

*372-373: this sentence should be reworded – Alk" is not a process. The meaning of the term "lower concentrations of recently-upwelled remineralized CT" is not clear.*

We got rid of this sentence during our pruning of the conclusions section.

*375: the direct temperature effect is minimal. It is the other two factors that matter.*

We also got rid of that sentence entirely.

*382-383: this should be explained more clearly or removed, given that the direct temperature effect is minimal.*

We got rid of this sentence as well.

*C5132*

*Figure 6: the colorbar needs a label with units. The meaning is unclear for the sentence in the caption beginning "Due to the log scale..."*

We remade the figure without cutting off the label, and removed that sentence from the caption (we removed the 2<sup>nd</sup> set of panels for  $A_T$  and  $S$  because we didn't discuss them):

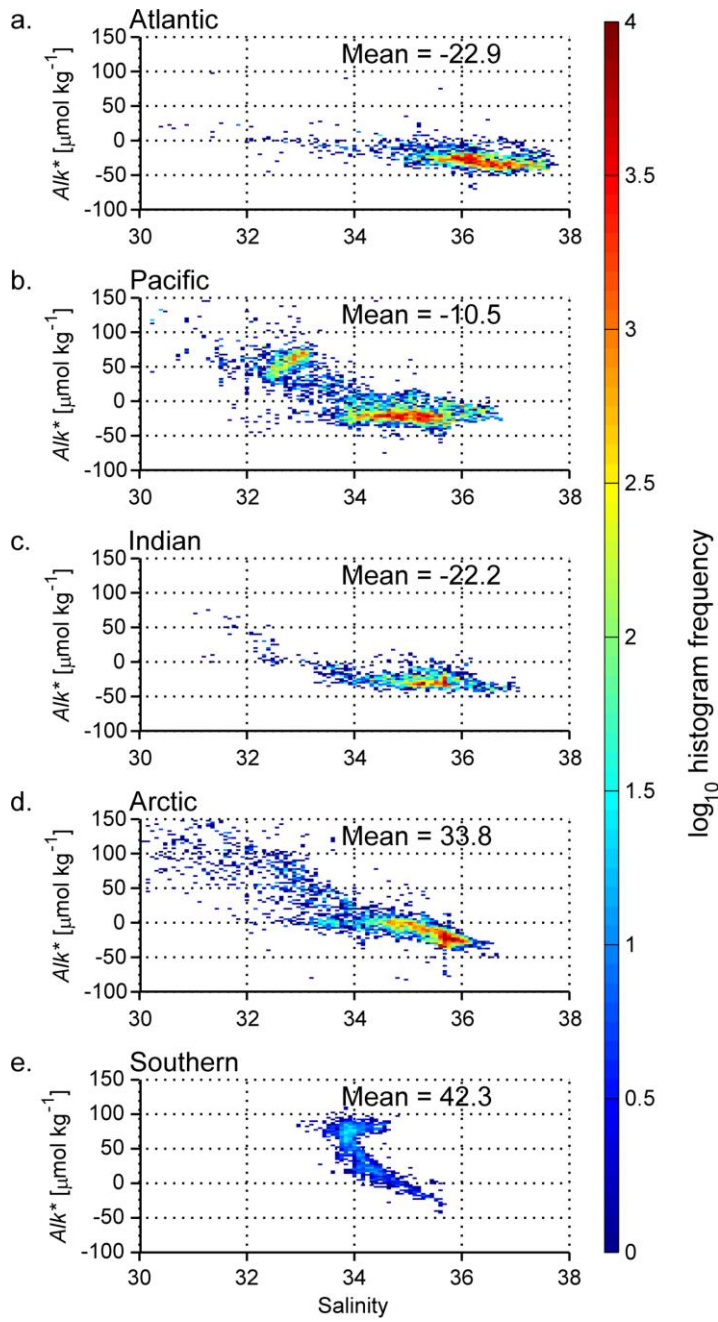


Figure 7: The red circles showing discharge volumes should be positioned closer to the point of entry of the rivers into the ocean.

I am hesitant to move these circles because I only have the locations as given in the Dai and Tenberth paper. It would be guesswork if I moved them closer to the ocean. Also, I believe the dots correspond to where the flow was estimated.

*References:*

Bates, Nicholas R., Jeremy T. Mathis, and Lee W. Cooper. "Ocean acidification and biologically induced seasonality of carbonate mineral saturation states in the western Arctic Ocean." *Journal of Geophysical Research: Oceans* (1978–2012) 114.C11 (2009).

Cooley, S. R., and P. L. Yager. "Physical and biological contributions to the western tropical North Atlantic Ocean carbon sink formed by the Amazon River plume." *Journal of Geophysical Research: Oceans* (1978–2012) 111.C8 (2006).

Cooley, S. R., et al. "Seasonal variations in the Amazon plume-related atmospheric carbon sink." *Global Biogeochemical Cycles* 21.3 (2007).

Jiang, Z. P., Tyrrell, T., Hydes, D. J., Dai, M., & Hartman, S. E. (2014). Variability of alkalinity and the alkalinity-salinity relationship in the tropical and subtropical surface ocean. *Global Biogeochemical Cycles*, 28(7), 729-742.

Mathis, Jeremy T., et al. "Storm-induced upwelling of high pCO<sub>2</sub> waters onto the continental shelf of the western Arctic Ocean and implications for carbonate mineral saturation states." *Geophysical Research Letters* 39.7 (2012).

Orr, James C., et al. "Anthropogenic ocean acidification over the twenty-first century and its impact on calcifying organisms." *Nature* 437.7059 (2005): 681-686.

Shaw, Emily C.; McNeil, Ben I. (2014) Seasonal variability in carbonate chemistry and air-sea CO<sub>2</sub> fluxes in the southern Great Barrier Reef. *MARINE CHEMISTRY* Volume: 158 Pages: 49-58 Published: JAN 20 2014

Tynan, Eithne, Toby Tyrrell, and Eric P. Achterberg. "Controls on the seasonal variability of calcium carbonate saturation states in the Atlantic gateway to the Arctic Ocean." *Marine Chemistry* 158 (2014): 1-9.

Williams, Richard G., and Michael J. Follows. *Ocean dynamics and the carbon cycle: Principles and mechanisms*. Cambridge University Press, 2011.

Yamamoto-Kawai, Michiyo, et al. "Aragonite undersaturation in the Arctic Ocean: effects of ocean acidification and sea ice melt." *Science* 326.5956 (2009): 1098-1100.

Zeebe, Richard E., and Dieter Wolf-Gladrow. *CO<sub>2</sub> in Seawater: Equilibrium, Kinetics, Isotopes: Equilibrium, Kinetics, Isotopes*. Elsevier, 2001.

*Interactive comment on Biogeosciences Discuss., 11, 11139, 2014.*

## Response to Reviewer #4

I have embedded specific responses to Reviewer #4's detailed and helpful comments below. Reviewer comments are in italicized text and my responses are in plain text. Excerpts from the revised text are in bold.

-Brendan and coauthors

### Reviewer #4

Comments on *Biogeosciences Discuss.*, 2014-354: "Processes determining the marine alkalinity and carbonate saturation distributions" by **B. R. Carter et al.**

#### I. General comments

*In this manuscript, the authors introduce a composite tracer  $Alk^*$  to study the process determining the marine alkalinity and calcium carbonate saturation distributions. The authors present the global distributions of  $Alk^*$  and estimate the riverine AT budget for different ocean basins. On regional scale, the authors highlight the high  $Alk^*$  near river mouths due to riverine input and low  $Alk^*$  in the Red Sea due to biological precipitation of  $CaCO_3$ . For the variability of carbonate saturation state, the authors define a metric to evaluate the importance of various controlling factors. Overall, the subject of this manuscript meets the general interest of *Biogeosciences* and I support the publication of this work after a moderate modification. Please see below for my detailed comments.*

#### II. Specific comments

*1. p11141, line 18-21: "The marine AT distribution is affected by the cycling of carbonate, freshwater, and organic matter, so we develop the quasi-conservative tracer  $Alk^*$  to isolate the influences carbonate cycling."*

Variations of alkalinity in the ocean are mainly controlled by the following processes: 1) mixing between different water masses, (2) precipitation and evaporation, (3) production and remineralization of organic matter, (4) precipitation and dissolution of  $CaCO_3$ , (5) external sources such as riverine input, underground water, hydrothermal vent fluids, (6) redox reactions in anaerobic environment [Chen, 2002]. By integrating the concept of potential alkalinity, the tracer  $Alk^*$  is not affected by production and remineralization of organic matter (process 3). In addition, the influence of precipitation and evaporation (process 2) is removed by using the salinity-normalization method of Robbins (2001). On general,  $Alk^*$  is primarily affected by mixing (process 1), precipitation and dissolution of  $CaCO_3$  (process 4), riverine input (process 5). However, it should be mentioned that, in some special marine environments, the contributions of hydrothermal vent fluids, and redox reactions may be significant. In these cases,  $Alk^*$  is no longer a good "tracer to isolate the influences of carbonate cycling".

We now explicitly mention other anaerobic redox processes throughout the paper, and include a reworded version of the caution suggested above. We feel confident implying  $Alk^*$  removes the

majority of the influence of non-sedimentary redox reactions since potential alkalinity does adjust for denitrification, nitrate is the first of many electron acceptors to be utilized in anoxic environments, and nitrate is almost never fully depleted outside of sediments.

**6. It is however affected by anaerobic redox reactions (Chen, 2002).**

**We are primarily interested calcium carbonate cycling, item 3 in our list. In section 2 of this paper we therefore define a tracer we call  $Alk^*$  that removes the majority of the influences of organic matter cycling (item 4), freshwater cycling (item 2), and non-sedimentary anaerobic redox reactions (item 6) while still mixing conservatively, remaining insensitive to gas exchange, and responding to calcium carbonate cycling.**

...later...

**The influence of organic matter cycling on  $A_T$  is due primarily to the biologically-driven marine nitrogen cycle. Nitrate uptake for anaerobic denitrification and the production of amino acids occurs in an ~1:1 mole ratio with the release of molecules that increase  $A_T$  (Chen 2002).**

...later...

**However, hydrothermal vent fluid and non-denitrification anaerobic redox chemistry may substantively affect alkalinity distributions in some marine environments.  $Alk^*$  distributions could not be attributed purely to calcium carbonate cycling in these locations.**

*7. p11142, lines 7-19.*

*Please revise these sentences for a more accurate description of nitrogen cycle and its influence on alkalinity.*

*The three reaction equations here are questionable (e.g., nitrification starts from  $NH_3$  or  $NH_4^+$  in R1, R2 gives unrealistic product  $O_2$  in denitrification). These equations are not really useful for the following discussion and I suggest to remove them. If the authors want to keep these equations, please refer to the equations by Wolf-Gladrow et al. [2007]*

We have removed these equations and now refer to (Wolf-Gladrow et al., 2007) here. The revised text is provided as part of the response to the last point (beginning with “**The influence...**”)

*p11144, Eqs. 3-5*

*The global mean passive conservative potential alkalinity ( $AP^C$ ) is subtracted from potential alkalinity ( $AP$ ) to calculate  $Alk^*$  (Eqs. 3-5). Instead of using the global mean  $AP^C$ , is it better to use the mean surface  $AP^C$  in the low-latitude tropical open oceans? In these oligotrophic waters, influences of riverine input, convection and biogenic  $CaCO_3$  production are minor while most of alkalinity variability is controlled by precipitation and evaporation [Jiang et al., 2014; Millero*

*et al., 1998]. Therefore, it provides a better reference for defining  $Alk^*$ . In this way, positive  $Alk^*$  indicates alkalinity inputs (riverine inputs, upwelled deep water et al.) while negative  $Alk^*$  suggests alkalinity removal ( $CaCO_3$  precipitation et al.).*

These are indeed regions where evaporation and precipitation are more dominant of controls on alkalinity than elsewhere, but evaporation and precipitation play major roles in other regions as well. If we tailored our  $Alk^*$  definition to these regions, then our definition would be less well-suited for, for instance, the high latitudes where net precipitation dilutes waters enriched in alkalinity from upwelling and rivers. It seems to us that the most balanced definition is obtained by using the global volume-weighted surface mean value.

*p11144, lines 14-24.*

*The authors discuss the difference between  $Alk^*$  and the typical salinity-normalized result (sAP). The reasons why "sAP does not mix conservatively, has a variable response to carbonate production, and yields an undefined value for a riverine end-member with zero salinity and non-zero AP" and "the non-linearity of sAP" are discussed in detailed by Jiang et al. [2014].*

This recent paper was unfamiliar to me. We now cite this paper, which does indeed discuss this topic at length, and use it to justify pushing more of our analysis of the  $Alk^*$  salinity normalization approach (and one figure) into supplementary material.

**In Supplementary Materials document SC we demonstrate that  $Alk^*$  mixes conservatively, and briefly contrast  $Alk^*$  to traditionally normalized potential alkalinity which does not mix conservatively (Jiang et al., 2014).**

### *3. p11145- 11146, section 3.1*

*This section is not well-organized and Figs. 2-5 need more explanations. Consider to discuss the surface distribution (Fig. 2&3) in one paragraph and discuss the vertical gradient (Fig. 4&5) in the second paragraph.*

We reorganized this section in keeping with this suggestion and R3's comments. We hope the new presentation is easier to read. We shortened the discussion in lieu of dividing discussion of the surface and vertical gradient figures into two paragraphs.

**The phosphate (Fig. 2d) and  $Alk^*$  (Fig. 2c) distributions are similar at the surface. They are also similar at depth. Figures 3 and 4 show zonally-averaged gridded depth sections of  $Alk^*$  and phosphate.  $Alk^*$  and phosphate concentrations are low in the deep Arctic Ocean (Figs. 3d, and 4d), intermediate in the deep Atlantic Ocean (Figs. 3a and 4a), and high in the deep North Pacific (Figs. 3b and 4b) and deep North Indian (Figs. 3c and 4c) Oceans.  $Alk^*$  and phosphate distributions are similar because similar processes shape them: the hard and soft tissue pumps transport  $A_T$  and phosphate, respectively, from the surface to depth. The "oldest" water therefore has the highest net phosphate and  $Alk^*$  accumulation. High surface phosphate and  $Alk^*$  in the Southern Ocean and North Pacific in Figs. 2, 3,**

**and 4 are due to upwelled old deep waters.**

4. *“The similarity between phosphate and Alk\* distributions suggests that Alk\* captures the portion of AT that varies in response to biological cycling as the hard parts of marine organisms.” p11145, lines 23-24*

*This statement is not really true and need more explanations. Although the surface ocean Alk\* and phosphate have the same sources (upwelled deep water enriched in Alk\* and nutrient, riverine inputs), they are removed by different biological activities. Production of particle organic carbon (POC) decreases phosphate but has no effect on changing Alk\*. In contrast, precipitation of CaCO<sub>3</sub> decreases Alk\* without changing phosphate. As a result, the low surface concentrations of phosphate and Alk\* in the low-latitude open ocean are due to the weak convention and low biological productions of POC and CaCO<sub>3</sub>. The high concentrations of phosphate and Alk\* are generally in the high-nutrient low-chlorophyll (HNLC) regions, which is mainly due to the strong convention and low productions of POC and CaCO<sub>3</sub>. On the other hand, the surface concentrations of phosphate and Alk\* are related to the ratio of CaCO<sub>3</sub>/POC production (the rain ratio). Given the same initial condition, high rain ratio would result in relatively low Alk\* and high phosphate, and vice versa.*

We reworded this sentence, and clarified our meaning:

**Alk\* and phosphate distributions are similar because similar processes shape them: the hard and soft tissue pumps transport A<sub>T</sub> and phosphate, respectively, from the surface to depth.**

5. *Section 3.3:*

*Although the Amazon is the largest AT source, its Alk\* is relatively low. Therefore, the Amazon is not the best example to show the riverine Alk\*. I don't find Fig. 7 and the discussion on winter-summer difference (p11148, line 19 - p11149, line 2) are closed related to the main objectives of this study.*

In keeping with this and other reviewer comments, we shortened this discussion.

*The third paragraph (p11149, lines 15-30) only presents the estimates of the rivrine Alk\*. It should be moved to section 3.2 (constructing the riverine AT budget for ocean basins) or moved to supplement.*

We removed this paragraph.

8. *The authors define surface ocean as the top 50m of water column. It seems that 50m is a little bit deep. Normally, it is 20m depth in the (sub)tropics and 30m depth at high latitudes [Lee et al., 2006]. Meanwhile, the boundary between the Atlantic and the Arctic defined by the authors (40°N) seems a little bit south?*

We changed our Alk\* definition to rely upon to the top 20 m since evaporation and precipitation happen at the surface... however, we didn't update our section 4 calculations to

a shallower depth because the mean mixed layer depth in the Holte et al. (<http://mixedlayer.ucsd.edu/>) climatology is ~60 m. The 40°N parallel is indeed fairly far south as far as most conventions for the Arctic/Atlantic. However, the biogeochemical fronts separating the high latitude Atlantic and the North Atlantic Gyre appear to fall closer to this cutoff.

9. *Section 4.2, p11153, lines 13-25:*

$S2 = [Ca^{2+}] [CO_3^{2-}] / K'_{sp}$ , any factor affecting  $[Ca^{2+}]$ ,  $[CO_3^{2-}]$ , or  $K'_{sp}$  can modulate S2.

*Why only CT is mentioned in the discussions here?*

The discussion in this section is limited to how the well-equilibrated case differs from the atmospherically-isolated case. The other factors controlling calcite saturation besides  $C_T$  behave in essential the same ways in these two cases. We had originally included a discussion of the various factors that control calcite saturation, but cut it for brevity.

10. *Conclusions:*

*This section is too long. Please provide more concise conclusions.*

We have truncated this section considerably (except where Reviewer #1 requested more detail on future plans).

**III. Technical corrections**

*“carbonate saturation” => calcium carbonate saturation throughout the manuscript.*

Changed

*p11140, line 20:*

*“to isolate the influences carbonate” => to isolate the influences of carbonate*

Changed

*p11142, line 5:*

*“while still mixing” => while still mixing conservatively*

Added

*p11145, lines 21-22:*

*“The similarity of the AT and salinity distributions demonstrates the strong influence of freshwater cycling on the surface marine AT distribution [Jiang et al., 2014; Millero et al., 1998]”. Please add references here.*

Added

p11146, line 1-2

*“The Alk\* distribution has a broadly similar explanation to the phosphate distribution.”*

*is a repetitive sentence. Delete it.*

Deleted

p11149, line 27:

*“into the Yellow Sea” => into the East China Sea*

This paragraph was removed.

p11152, line 21:

*“alongside the ... values”. Please correct the symbols in this sentence.*

Fixed

p11154, lines 17-18:

*“A plot of Alk\* against salinity reveals the large AT input from the Amazon River”.*

*This sentence come from nowhere (which plot?).*

We removed this sentence.

Fig. 6:

*The color (the numbers of measurements) in this figure is not really useful.*

As we argued in our response to R3, we feel the color plays the important role of showing which regions of the plot represent common water masses vs. which simply have at least one measurement representing them. We’ve added verbiage (in red) to highlight this distinction:

**The Alk\* elevation associated with upwelled water is most visible in Fig. 5e where Upper Circumpolar Deep Water upwelling near the Polar Front results in high-frequency (i.e. warm colored) bins at high-Alk\*. Similarly, the high-frequency Alk\* bins in Fig. 5b with salinity between 32.5 and 33.5 are from the North Pacific Subpolar Gyre, and are also due to upwelled old high-Alk\* water (cf. the Si\* tracer in Sarmiento et al. (2004)). River water contributions can be most easily seen in a scattering of low-frequency (cool colored) very high-Alk\* and very low-salinity bins in the Arctic Ocean.**

#### **References:**

Chen, C.-T. A. (2002), Shelf-vs. dissolution-generated alkalinity above the chemical lysocline, *Deep Sea Research Part II: Topical Studies in Oceanography*, 49(24–25), 5365-5375, doi: 10.1016/S0967-0645(02)00196-0.

Jiang, Z.-P., T. Tyrrell, D. J. Hydes, M. Dai, and S. Hartman (2014), Variability of alkalinity and alkalinity-salinity relationship in the tropical and subtropical surface ocean, *Global Biogeochemical Cycles*, 28, 729-742.

Lee, K., L. T. Tong, F. J. Millero, C. L. Sabine, A. G. Dickson, C. Goyet, G. H. Park, R. Wanninkhof, R. A. Feely, and R. M. Key (2006), Global relationships of total alkalinity with salinity and temperature in surface waters of the world's oceans, *Geophysical Research Letters*, 33(19), L19605, doi: 10.1029/2006gl027207.

Millero, F. J., K. Lee, and M. Roche (1998), Distribution of alkalinity in the surface waters of the major oceans, *Marine Chemistry*, 60(1-2), 111-130.

Wolf-Gladrow, D. A., R. E. Zeebe, C. Klaas, A. Kortzinger, and A. G. Dickson (2007), Total alkalinity: The explicit conservative expression and its application to biogeochemical processes, *Marine Chemistry*, 106(1-2), 287-300, doi: 10.1016/j.marchem.2007.01.006

| Processes determining the marine alkalinity and calcium carbonate ~~mineral~~ saturation distributions

Carter, B. R.<sup>1</sup>, J. R. Toggweiler<sup>2</sup>, R. M. Key<sup>1</sup>, and J. L. Sarmiento<sup>1</sup>

---

Brendan Carter ([brcarter@princeton.edu](mailto:brcarter@princeton.edu))

J.R. Toggweiler ([Robbie.Toggweiler@noaa.gov](mailto:Robbie.Toggweiler@noaa.gov))

Robert M. Key ([key@princeton.edu](mailto:key@princeton.edu))

Jorge L. Sarmiento ([jls@princeton.edu](mailto:jls@princeton.edu))

## 1 Abstract

2 We introduce a composite tracer,  $Alk^*$ , that has a global distribution primarily determined  
 3 by  $CaCO_3$  precipitation and dissolution.  $Alk^*$  ~~highlights~~ is also affected by riverine alkalinity  
 4 ~~plumes that are due to from~~ dissolved ~~calcium~~ terrestrial carbonate ~~from land~~ minerals. We  
 5 estimate the Arctic receives approximately twice the riverine alkalinity per unit area as the  
 6 Atlantic, and 8 times that of the other oceans. Riverine inputs broadly elevate  $Alk^*$  in the Arctic  
 7 surface and particularly near river mouths. Strong net carbonate precipitation ~~lowers basin mean~~  
 8 ~~results in low  $Alk^*$  in subtropical gyres, especially in the~~ Indian and Atlantic  ~~$Alk^*$ , while~~  
 9 ~~upwelling~~ Oceans. Upwelling of dissolved  $CaCO_3$  rich deep ~~waters~~ water elevates Northern  
 10 Pacific and Southern Ocean  $Alk^*$ . We use the  $Alk^*$  distribution to estimate the ~~carbonate~~ calcite  
 11 saturation variability resulting from  $CaCO_3$  cycling and other processes. We show regional  
 12 ~~variations~~ differences in surface ~~carbonate~~ calcite saturation are due to the effect of temperature  
 13 ~~changes driving differences on~~  $CO_2$  ~~fluxes~~ solubility and, to a lesser extent, differences in  
 14 freshwater content and air-sea disequilibria. ~~The variations in net calcium carbonate cycling-~~  
 15 ~~Calcium carbonate cycling plays a tertiary~~ revealed by  $Alk^*$  play a comparatively minor role.  
 16 ~~Monitoring the  $Alk^*$  distribution would allow us to isolate the impact of acidification on~~  
 17 ~~biological calcification and remineralization.~~

Formatted: Font: Italic

## 19 1. Introduction

20 Our goal is to use high-quality total alkalinity ( $A_T$ ) observations to examine the effects of  
 21 calcium carbonate cycling on marine  $A_T$  and calcium carbonate ~~mineral~~-saturation states. ~~The~~  
 22 ~~marine  $A_T$  distribution~~ This study is affected ~~motivated in part~~ by the cycling of ocean  
 23 acidification. With marine calcite saturation decreasing due to anthropogenic carbon uptake, it is

Formatted: Pattern: Clear

Formatted: Pattern: Clear

24 ~~important to understand the degree to which carbonate, freshwater, and organic matter, so we~~  
 25 ~~develop the quasi-conservative tracer  $Alk^*$  to isolate the influences cycling impacts calcite~~  
 26  ~~saturations.~~

Formatted: Pattern: Clear

27 ~~Marine calcium carbonate cycling.  $Alk^*$  is estimated by adjusting  $A_T$  to remove the~~  
 28  ~~influences of organic matter cycling, and then subtracting a salinity-based estimate of what the~~  
 29  ~~adjusted  $A_T$  would be if the net influence of- includes both internal and external calcium~~  
 30  ~~carbonate cycling. Internal cycling were uniform in the ocean. refers to net formation of 67-300~~  
 31  ~~$\times 10$  Tmoles  $A_T$   $yr^{-1}$  worth of calcium carbonate (Berelson et al., 2007) in the surface ocean and~~  
 32  ~~net dissolution of most of this calcium carbonate at depth. External marine carbonate cycling~~  
 33  ~~refers to inputs of carbonate minerals dissolved in rivers, sediment pore waters, hydrothermal~~  
 34  ~~vent fluids, and submarine groundwater discharge, and loss due to biogenic carbonate mineral~~  
 35  ~~burial and authigenic mineralization in sediments. Rivers add 33 Tmoles  $A_T$   $yr^{-1}$  worth of~~  
 36  ~~dissolved bicarbonate to the ocean (Cai et al., 2008). Wolery and Sleep (1988) estimate~~  
 37  ~~hydrothermal vents add an additional 6.6 Tmoles  $A_T$   $yr^{-1}$ , though deVilliers (1998) argues the~~  
 38  ~~hydrothermal contribution may be as high as 30 Tmoles  $A_T$   $yr^{-1}$ . Submarine groundwater~~  
 39  ~~discharge is poorly constrained, but is thought to exceed riverine inputs in some areas (Moore,~~  
 40  ~~2010).~~

Field Code Changed

41 We investigate calcium carbonate cycling using the global  $Alk^*A_T$  distribution ~~usingin~~ a  
 42 dataset we created by merging the PACIFICA (Suzuki et al., 2013), GLODAP, and CARINA  
 43 discrete data products (Key et al. 2004; 2010; Velo et al., 2009). We have combined and gridded  
 44 these data products using methods detailed in Supplementary Materials document SA. We use  
 45 our gridded dataset in some calculations to limit sampling biases and to enable us to make  
 46 volume-weighted mean property estimates.

~~This study is motivated in part by ocean acidification. With marine carbonate saturation decreasing due to anthropogenic carbon uptake, it is important to understand the degree to which carbonate cycling impacts marine carbonate saturations and vice versa. In this paper we use  $Alk^*$  to show net carbonate precipitation and dissolution variability is not a dominant control for carbonate saturation variability. We will address the converse question in future work with  $Alk^*$ .~~

~~We derive  $Alk^*$  in section 2. In section 3 we discuss processes that govern the  $Alk^*$  distribution globally, by ocean basin, and regionally. In section 4 we define a metric to quantify the influence of various processes over the marine calcium carbonate saturation state. We use this metric with our gridded dataset and  $Alk^*$  to determine the relative importance of the various controls in the ocean and at the ocean surface. We summarize in section 5.~~

## ~~2. The $Alk^*$ tracer~~

Dickson (1981) defines total alkalinity as the concentration excess “of proton acceptors formed from weak acids ( $pK \leq 4.5$ ) relative to proton donors (weak bases with  $pK > 4.5$ )” at a reference temperature, pressure, and ionic strength.  $A_T$  can be thought of as a measure of how well buffered seawater is against changes in pH. This operational definition gives  $A_T$  (expressed in  $\text{mol kg}^{-1}$ ) several properties that make it an especially useful carbonate system parameter for examining carbonate cycling:

1. It mixes conservatively,
2. ... and is therefore diluted and concentrated linearly by evaporation and precipitation.
3. It responds in predictable ways to calcium carbonate cycling.
4. ... as well as organic matter formation and remineralization.
5. It is not changed by the air-sea exchange of heat or carbon dioxide.

Formatted: Indent: First line: 0"

Field Code Changed

Field Code Changed

6. It is however affected by anaerobic redox reactions (Chen, 2002).

We are primarily interested ~~in the calcium carbonate cycling of biogenic carbonates~~, item 3 in our list. ~~It is~~ In section 2 of this paper we therefore ~~useful to~~ define a tracer we call  $Alk^*$  that removes the majority of the influences of organic matter cycling (item 4) ~~and~~, freshwater cycling (item 2), and non-sedimentary anaerobic redox reactions (item 6) while still mixing conservatively, remaining insensitive to gas exchange, and responding to calcium carbonate cycling. In section 3 we discuss processes that govern the  $Alk^*$  distribution globally, by ocean basin, and regionally. In section 4 we define a metric to quantify the influence of various processes ~~linearly~~ on the marine calcite saturation state. We use this metric with our gridded dataset and  $Alk^*$  to determine the relative importance of the various controls on calcite saturation in the ocean and at the ocean surface. We summarize our findings in section 5.

## 2. The $Alk^*$ tracer

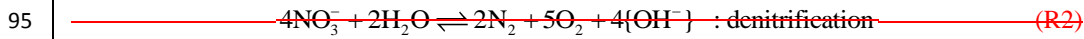
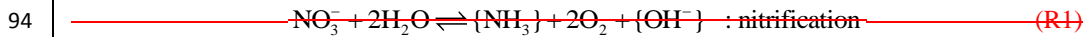
In defining  $Alk^*$ , we take advantage of the potential alkalinity (Brewer et al., 1975) concept to remove the majority of the influence of organic matter ~~formation~~ cycling and denitrification, and use a specific salinity normalization scheme (Robbins 2001) to remove the influence of freshwater cycling. We detail the  $Alk^*$  definition and the reasoning behind it in this section.

The influence of organic matter cycling on  $A_T$  is due primarily to the biologically-driven marine nitrogen cycle. ~~We provide simplified~~ Nitrate uptake for anaerobic denitrification and the production of amino acids occurs in an ~1:1 mole ratio with the release of molecules that increase  $A_T$  (Chen 2002). Similarly, nitrate from fixation of nitrogen ~~cycle reactions (R1-R3)~~ gas and remineralization of amino nitrogen is released in a 1:1 mole ratio with proton-accepting

Formatted: Indent: First line: 0"

Formatted: Font: Bold

93 ~~basesacids~~ that ~~represent a positive contribution fortitrate away~~  $A_T$  ~~indicated with curly brackets.~~



97 ~~Organic matter incorporates the ammonia ( $\text{NH}_3$ ) produced by nitrification, making it~~

Formatted: Indent: First line: 0.5"

98 ~~slightly alkaline (Hernández Ayon(Wolf-Gladrow et al., 2007). However, organic matter is~~

Formatted: Pattern: Clear (White)

99 ~~typically remineralized in situ or exported, so it is generally assumed that the net uptake of~~

100 ~~nitrate corresponds to a 1:1 release of proton acceptors in these reactions (e.g.  $\text{OH}^-$ ).~~ This

101 observation led Brewer ~~and Goldman (1976~~et al. (1975) to propose the idea of “potential

102 alkalinity” as the sum of  $A_T$  and nitrate with the aim of creating a tracer that responds to the

103 cycling of calcium ~~carbonate~~carbonates without changing in response to organic matter cycling.

104 Feely et al. (2002) since used a variant that relies on the empirical relationship between dissolved

105 calcium concentrations,  $A_T$ , and nitrate determined by Kanamori and Ikegami (1982). This

106 variant has the advantage of implicitly accounting for the  $A_T$  changes created by the exchange of

107 numerous other components of marine organic matter besides nitrate (e.g. sulfate and

108 phosphate). ~~While the empirical relationship measured may be specific to the elemental ratios of~~

109 ~~the North Pacific, Wolf-Gladrow et al. (2007) provide a theoretical derivation from Redfield~~

110 ~~ratios and obtain a similar value. We also~~We thus use the ratio found by Kanamori and Ikegami

111 (1982) to define potential alkalinity ( $A_p$ ).

112  ~~$A_p = A_T + 1.26 * [\text{NO}_3^-]$~~   $A_p = A_T + 1.26 * [\text{NO}_3^-]$  (1)

Field Code Changed

113 While the empirical ratio of 1.26 may be specific to the elemental ratios of the North Pacific,

114 Wolf-Gladrow et al. (2007) provide a theoretical derivation from Redfield ratios and obtain a

115 similar value of 1.36.

116 The sensitivity of the  $A_T$  distribution to freshwater cycling is due primarily to the dilution  
 117 or concentration of the large background  $A_T$  fraction that does not participate in carbonate  
 118 cycling on timescales of ocean mixing. ~~However, freshwater sources such as ground water and  
 119 river water can also be rich in dissolved carbonates and represent an oceanic  $A_T$  source that we  
 120 consider with our tracer. We therefore use a salinity normalization similar to the approach of  
 121 Robbins (2001) to remove the large background fraction of surface  $A_T$  without removing  $A_T$  from  
 122 dissolved carbonates in river water and groundwater. We accomplish this by subtracting our  
 123 estimate of the passive conservative potential alkalinity ( $A_p^C$ ), that we define This background  
 124 fraction behaves conservatively, so we call it conservative potential alkalinity ( $A_p^C$ ) and estimate  
 125 it directly from salinity as:~~

$$126 \quad \overline{A_p^C} = \overline{S} \frac{\overline{A_p}}{\overline{S}} \quad \overline{A_p^C} = \overline{S} \frac{\overline{A_p}}{\overline{S}}$$

127 Here, terms with a bar are reference values chosen as the mean value for those properties in the  
 128 top 5020 meters of the ocean. We obtain a volume-weighted surface  $\overline{A_p}$   $\overline{A_p}$  (2305  $\mu\text{mol kg}^{-1}$ ) to  
 129  $\overline{S}$   $\overline{S}$  (34.71) ratio of 66.440  $\mu\text{mol kg}^{-1}$  from our gridded dataset. The mean surface values are  
 130 chosen ~~to~~ in an effort to best capture the impact of freshwater cycling where precipitation and  
 131 evaporation occur.

132 Robbins (2001) showed that subtracting an estimate of the conservative portion of a  
 133 tracer, such as  $A_p^C$ , produces a salinity-normalized composite tracer that mixes conservatively.

134 This scheme also retains the 2:1 change of  $A_T$  to dissolved inorganic carbon ( $C_T$ ) with carbonate  
 135 cycling. We follow this approach in our definition of  $Alk^*$ . In Supplementary Materials

Field Code Changed

Field Code Changed  
(2)

Field Code Changed

Field Code Changed

Formatted: Indent: First line: 0.5"

Field Code Changed

document SB; we estimate this approach removes 97.5% of the influence of freshwater cycling on potential alkalinity and reduces the influence of freshwater cycling on  $Alk^*$  to less than 1% of the  $Alk^*$  variability. In Supplementary Materials document SC we demonstrate that  $Alk^*$  mixes conservatively, and briefly contrast  $Alk^*$  to traditionally normalized potential alkalinity which does not mix conservatively (Jiang et al., 2014).

In total, we define  $Alk^*$  as the deviation of potential alkalinity from  $A_p^C$ ,  $A_p^C$ .

$$Alk^* \equiv A_p - A_p^C \quad Alk^* \equiv A_p - A_p^C \quad (3) \quad (3)$$

$$\equiv A_p - \frac{A_p}{S} S \quad \equiv A_p - \frac{A_p}{S} S \quad (4) \quad (4)$$

$$\equiv A_p - 66.4 \times S \text{ } \mu\text{mol kg}^{-1} \quad \equiv A_p - 66.4 \times S \quad (5) \quad (5)$$

where  $Alk^*$  has alkalinity the same units as  $A_T$  ( $\mu\text{mol kg}^{-1}$ ). The  $Alk^*$  distribution is attributable primarily to carbonate cycling plus the small residual variation due to freshwater cycling that is not removed by subtracting  $A_p^C$ . Mean global surface  $Alk^*$  is zero by definition, and negative  $Alk^*$  is possible when potential alkalinity is less than expected from salinity. For reference, more than 95% of our gridded  $Alk^*$  dataset falls between -35 and 220  $\mu\text{mol kg}^{-1}$   $A_p^C$ . However, hydrothermal vent fluid and non-denitrification anaerobic redox chemistry may substantially affect alkalinity distributions in certain marine environments, and  $Alk^*$  distributions could not be attributed purely to internal and external calcium carbonate cycling in these locations.

$Alk^*$  mixes conservatively (demonstrated in Supplementary Materials document SC), retains the 2:1 change of  $A_T$  to dissolved inorganic carbon ( $C_T$ ) with formation or dissolution of calcium carbonate, and preserves dissolved carbonate alkalinity entering the ocean in river water. By contrast, typical salinity normalization (e.g.  $sA_p$ , which multiplies potential alkalinity by the ratio between the *in situ* salinity and reference salinity) does not mix conservatively, has a variable response to carbonate production, and yields an undefined value for a riverine end-

Field Code Changed

Field Code Changed

Field Code Changed

157 ~~member with zero salinity and non-zero  $A_p$ . The  $Alk^*$  and  $sA_p$  distributions are broadly similar~~  
 158 ~~despite these differences in approach, though discrepancies between them are pronounced where~~  
 159 ~~there are large concentrations of riverine water. Figure 1 shows differences between individual~~  
 160  ~~$sA_p$  estimates and the global mean estimate  $\overline{sA_p}$  against the differences between individual  $Alk^*$~~   
 161 ~~estimates and the global mean estimate  $\overline{Alk^*}$ . This figure reveals that the non-linearity of  $sA_p$~~   
 162 ~~can bias estimates high by  $>2000 \mu\text{mol kg}^{-1}$ .~~

163 Mean global surface  $Alk^*$  is zero by definition, and thus  $Alk^*$  can have negative as well  
 164 as positive values. For reference, more than 95% of our gridded  $Alk^*$  dataset falls between  $-35$   
 165 and  $220 \mu\text{mol kg}^{-1}$ .

166

### 167 3. $Alk^*$ distributions

168 ~~The  $Alk^*$  distribution is affected by both internal and external marine carbonate cycling.~~  
 169 ~~Internal cycling is due to net carbonate formation in the surface ocean and net dissolution at~~  
 170 ~~depth. External cycling is due to  $Alk^*$  input by rivers and hydrothermal vent fluids balanced by~~  
 171 ~~loss due to burial of biogenic carbonates and authigenic mineralization in sediments. Before~~  
 172 ~~showing the global  $Alk^*$  distribution, we briefly provide background on  $A_p$  inputs to the ocean.~~

173 ~~The dominant source of  $Alk^*$  to the ocean is dissolved carbonate minerals in river water,~~  
 174 ~~ground water, and hydrothermal vent fluid. For river water with a salinity of 0,  $Alk^*$  equals the~~  
 175 ~~potential alkalinity. We consider  $Alk^*$  distributions globally, by ocean basin, and regionally in~~  
 176 ~~the context of sources and sinks of the tracer both globally and regionally. We pay special~~  
 177 ~~attention to riverine  $Alk^*$  because it is easily identified where it accumulates near river mouths.~~

178 ~~This averages around  $1100 \mu\text{mol kg}^{-1}$  globally (Cai et al., 2008), but is greater than  $3000$~~   
 179  ~~$\mu\text{mol kg}^{-1}$  for some rivers (Beldowski et al., 2010). Evidence suggests that riverine  $A_p$  is~~

Formatted: Tab stops: 3.25", Centered + 6.5", Right

Formatted: Tab stops: Not at 3.25" + 6.5"

180 ~~increasing due to human activities (Kaushal et al., 2013).~~

181 ~~Wolery and Sleep (1988) estimate hydrothermal vents add  $0.04 \text{ Pg C yr}^{-1}$  of carbonate to~~  
 182 ~~the ocean. This is one fifth of the  $0.2 \text{ Pg C yr}^{-1}$  riverine source (Cai et al., 2008), though~~  
 183 ~~deVilliers (1998) suggested that the hydrothermal contribution may be as high as  $0.18 \text{ Pg C yr}^{-1}$ .~~

184 Formatted: Indent: First line: 0.5"

### 185 3.1 Global distribution of $Alk^*$

186 ~~We map Figure 1 maps surface  $Alk^*$  (top 50 m) at the measurement stations. We provide~~  
 187 ~~this figure to show where we have viable  $Alk^*$  estimates and to demonstrate that our gridded data~~  
 188 ~~product adequately captures the measured  $Alk^*$  distribution. Figure 2 maps gridded global~~  
 189 ~~surface  $A_T$ , salinity,  $Alk^*$ , and phosphate distributions and mask the regions that are lacking data~~  
 190 ~~in Fig. 2. Figure 3 shows the surface (top 50 m) distribution of  $Alk^*$  at the measurement stations.~~  
 191 ~~1.~~

192 The similarity of the  $A_T$  (Fig. 2a) and salinity (Fig. 2b) distributions demonstrates the  
 193 strong influence of freshwater cycling on the surface marine  $A_T$  distribution. (see also: Millero et  
 194 al. 1998, Jiang et al., 2014). The ~~similarity~~ ~~dissimilarity~~ between ~~phosphate~~  $Alk^*$  (Fig. 2c) and  
 195  $Alk^*$  ~~distribution~~ ~~salinity~~ (Fig. 2b) suggests ~~that  $Alk^*$  captures~~ ~~removes~~ the ~~portion~~ ~~majority~~ of  $A_T$   
 196 ~~that varies in response to biological cycling as this influence. The phosphate (Fig. 2d) and  $Alk^*$~~   
 197 ~~(Fig. 2c) distributions are similar at the hard parts of marine organisms. This similarity extends~~  
 198 ~~to surface. They are also similar at depth as well.;~~ Figures 3 and 4 and 5 show zonally-averaged  
 199 ~~gridded~~ depth sections of  $Alk^*$  and phosphate ~~from the gridded fields, respectively. The~~  
 200 ~~subtropical gyres have the lowest open ocean  $Alk^*$  in Figs. 2, 3, and 4.  $Alk^*$ .  $Alk^*$  and~~  
 201 ~~phosphate~~ concentrations are ~~high~~ ~~low~~ in ~~the deep~~ Arctic ~~surface, deep North Indian, Ocean (Figs.~~  
 202 ~~3d, and 4d), intermediate in the deep Atlantic Ocean (Figs. 3a and 4a), and high in the deep~~

Formatted: Font: Not Italic

203 ~~North Pacific (Figs. 3b and 4b) and deep North Pacific-Indian (Figs. 3c and 4c) Oceans. The~~  
 204 ~~Alk\* distribution has a broadly and phosphate distributions are similar explanation to because~~  
 205 ~~similar processes shape them: the phosphate distribution, hard and soft tissue pumps transport A<sub>T</sub>~~  
 206 ~~uptake to form calcium carbonate reduces and phosphate, respectively, from the surface Alk\*.~~  
 207 ~~Dissolution of these carbonates at to depth increases Alk\*.~~ The “oldest” water therefore has the  
 208 highest net phosphate and Alk\* accumulation. High surface phosphate and Alk\* in the Southern  
 209 Ocean and North Pacific ~~is in Figs. 2, 3, and 4 are~~ due to upwelled old deep waters.

210 Several qualitative differences between Alk\* and phosphate distributions are visible in  
 211 Figs. ~~2, 2c, 2d, 3, and 4, and 5~~. Surface phosphate is low in the Bay of Bengal and high in the  
 212 Arabian Sea, ~~(Fig. 2d)~~, while the opposite is true for Alk\* ~~\*(Fig. 2c)~~. ~~Also~~, Alk\* reaches its  
 213 highest surface concentration in the Arctic ~~(Figs. 2c and 3d)~~ where phosphate is not greatly  
 214 elevated ~~(Figs. 2d and 4d)~~. These surface differences are due to regional ~~river water riverine~~  
 215 Alk\* inputs (Section 3.3). ~~Another difference is that~~ Alk\* reaches a ~~maximamaximum~~ below  
 216 2000 m in all ocean basins except the Arctic, while phosphate maxima are above 2000 m. We  
 217 attribute the deeper Alk\* maxima to deeper dissolution of ~~carbonate minerals calcium carbonates~~  
 218 than organic matter remineralization. ~~Another exception is the higher~~ Finally, Alk\* values are  
 219 higher in the deep Indian Ocean than in the deep Pacific. This is likely due to elevated biogenic  
 220 carbonate export along the coast of Africa and in the Arabian Sea ~~found by (Sarmiento et al. (~~  
 221 ~~2002) and; Honjo et al. (~~ 2008).

222

### 223 3.2 Alk\* by ocean basin

224 In Fig. ~~65~~ we provide 2-D color histograms of discrete surface Alk\* and ~~A<sub>T</sub> vs.~~ salinity  
 225 measurements for the five major ocean basins ~~and indicate the~~. Figure 5 also provides volume-

Formatted: Font: Not Italic

Formatted: Pattern: Clear (White)

Formatted: Pattern: Clear (White)

226 ~~weighted~~ mean  ~~$A_T$~~  and gridded  $Alk^*$  for ~~discrete measurement data from~~ each basin. We attribute  
 227 the decrease in  $Alk^*$  as salinity increases—especially visible in ~~lower the low-salinity values bins~~  
 228 in the Arctic Ocean—(Fig. 5d)—to mixing between high- $Alk^*$  low-salinity river water and ~~the~~  
 229 ~~comparatively~~ low- $Alk^*$  high-salinity open ocean water. ~~Precipitation and Net precipitation in~~  
 230 ~~the tropics and net~~ evaporation in the ~~subtropical gyres subtropics~~ widens the histograms across a  
 231 ~~wide~~ range of salinities and alkalinities without affecting  $Alk^*$ . ~~in Figs. 5a, 5b, and 5c.~~ The  
 232  $Alk^*$  elevation associated with upwelled water is most visible in Fig. 6j5e where Upper  
 233 Circumpolar Deep Water upwelling near the Polar Front ~~produces a clump of results in high-~~  
 234 ~~frequency (i.e. warm colored) histogram bins at high-~~  $Alk^*$  ~~data lacking~~. Similarly, the ~~very~~  
 235 ~~low salinity tail characteristic of riverine input. The high~~ high-frequency  $Alk^*$  ~~measurements bins~~  
 236 in Fig. 6d5b with salinity between 32.5 and 33.5 are from the North Pacific Subpolar Gyre, and  
 237 are ~~also~~ due to upwelled old high- $Alk^*$  water (cf. the  $Si^*$  tracer in Sarmiento et al. (2004)). ~~River~~  
 238 ~~water contributions can be most easily seen in a scattering of low-frequency (cool colored) high-~~  
 239  ~~$Alk^*$  and low-salinity bins in the Arctic Ocean.~~

240 The surface Southern Ocean has the highest  $Alk^*$  followed by the Arctic, Pacific, ~~and the~~  
 241 Indian, and Atlantic. The high mean Southern Ocean  $Alk^*$  is due to upwelling. The high ~~mean~~  
 242 Arctic surface  $Alk^*$  is due to riverine input. The Atlantic and the Arctic together receive ~65%  
 243 of all river water (Dai and Trenberth, 2002). We construct a ~~riverine  $A_T$~~  budget for ~~terrestrial  $A_T$~~   
 244 ~~sources to~~ the various ~~surface~~ ocean basins using the following assumptions:

- 245 1. the  $A_T$  of 25 large rivers are as given by Cai et al. (2008),
- 246 2. the volume discharge rates of 200 large rivers are as given by Dai and Trenberth  
 247 (2002),
- 248 3. groundwater and runoff enter each ocean in the same proportion as river water from

249 these 200 rivers,

250 4. the  $A_T$  of all water types that we do not know from assumption 1. is the 1100  $\mu\text{mol}$   
 251  $\text{kg}^{-1}$  global mean value estimated by Cai et al. (2008), and

252 5.  $40^\circ\text{N}$  is the boundary between the Atlantic and the Arctic and  $40^\circ\text{S}$  is the boundary  
 253 between the Southern and the Atlantic Oceans (based upon the region of elevated  
 254 surface phosphate in Fig. 2d),

255 Our detailed budget is provided as Supplementary Materials file SD. We estimate 40% of  
 256 continentally derived  $A_T$  enters the Atlantic, 20% enters the Arctic, and 40% enters all remaining  
 257 ocean basins. These ocean areas represent 17%, 5%, and 78% of the total surface ocean area in  
 258 our gridded dataset respectively, so the Arctic receives approximately twice as much riverine  $A_T$   
 259 per unit area as the Atlantic, and 8 times the rest of the world ocean. The Atlantic has the lowest  
 260 ~~measured~~ open-ocean surface  $Alk^*$  value and the lowest basin mean surface  $Alk^*$  despite the  
 261 large riverine sources. The large riverine  $A_T$  input must therefore be more than balanced by  
 262 strong net calcium carbonate formation. The Indian Ocean ~~also~~ has acomparably low mean  
 263 surface  $Alk^*$  ~~that we attribute to strong net carbonate precipitation. The nearly zero mean~~  
 264 ~~surface Pacific  $Alk^*$  indicates that  $Alk^*$  supply from upwelling and a small~~ the Atlantic, but a  
 265 smaller riverine source ~~very nearly balances carbonate precipitation. Mean  $Alk^*$  is higher in the~~  
 266 Pacific than the Atlantic and Indian, even when neglecting the upwelling region north of  $40^\circ\text{N}$   
 267 ( $Alk^* = -16.5 \mu\text{mol kg}^{-1}$  when omitted). Considering the weak Pacific riverine input, this  
 268 suggests that, relative to other ocean basins, there are either larger  $Alk^*$  inputs from exchange  
 269 with other basins and deeper waters or smaller Pacific basin mean net calcium carbonate.

270

271 3.3 Riverine  $Alk^*$  regionally

272 River water has a high average  $Alk^*$  ( $1100 \mu\text{mol kg}^{-1}$ ), so carbonate-rich river discharge  
 273 can be seen as regionally elevated  $Alk^*$ . The total riverine  $A_T$  per unit drainage area varies with  
 274 the quantity of carbonate minerals found in the drainage region (Cai et al., 2008). The  $A_T$  load is  
 275 diluted by total discharge, so high discharge rivers (e.g. the Amazon and the Congo) often have  
 276 low  $Alk^*$ .

277 For river water with negligible salinity,  $Alk^*$  equals the potential alkalinity. This  
 278 averages around  $1100 \mu\text{mol kg}^{-1}$  globally (Cai et al., 2008), but is greater than  $3000 \mu\text{mol kg}^{-1}$   
 279 for some rivers (Beldowski et al., 2010). Evidence suggests that riverine  $A_T$  is increasing due to  
 280 human activities (Kaushal et al., 2013).

281 ~~The Amazon River is the largest single riverine marine  $A_T$  source. This river has low  $A_T$~~   
 282 ~~( $369 \mu\text{mol kg}^{-1}$  (Cai et al., 2008)), but has the largest water discharge volume of any river,~~  
 283 ~~exceeding the second largest—the Congo—by a factor of 5 (Dai and Trenberth, 2002).~~  
 284 ~~Consequently, the Amazon discharges approximately 50% more  $A_T$  per year than the river with~~  
 285 ~~the second largest  $A_T$  discharge, the Changjiang (Cai et al., 2008). The Amazon's influence can~~  
 286 ~~be seen as a region of abnormally low salinity and  $A_T$  in Fig. 2a and b. Despite the high~~  
 287 ~~discharge volume, the influence is only barely visible as a region of elevated  $Alk^*$  in Fig. 2c due~~  
 288 ~~to the comparatively low Amazon  $Alk^*$ . The Amazon's influence is perhaps most easily seen in~~  
 289 ~~the elevated  $Alk^*$  values in the lowest salinity data in Fig. 6b. Figure 7 provides a map of  $Alk^*$~~   
 290 ~~for this region scaled to show the influence of this low  $Alk^*$  river in the Northern Hemisphere (a)~~  
 291 ~~winter and (b) summer months. The higher  $Alk^*$  found for May through July is consistent with~~  
 292 ~~Moore et al. (1986)'s radium isotope based finding that 20–34% of the surface waters in this~~  
 293 ~~region are derived from Amazon during July versus 5–9% during December. However, if we~~  
 294 ~~assume the Atlantic seawater mixing with the Amazon outflow had an  $Alk^*$  of  $-35 \mu\text{mol kg}^{-1}$ ,~~

Formatted: Tab stops: Not at 3.25" + 6.5"

295 ~~these Amazon River water fractions would result in  $Alk^*$  of  $-15$  to  $0 \mu\text{mol kg}^{-1}$  in December~~  
296 ~~and  $45$  to  $100 \mu\text{mol kg}^{-1}$  in July. We see lower  $Alk^*$  values in our distribution and a smaller~~  
297 ~~disparity between winter and summer  $Alk^*$ , suggesting a smaller average Amazon influence for~~  
298 ~~the ocean's surface during both seasons than found by Moore et al. (1986). However, our~~  
299 ~~estimate does not account for any changes in calcium carbonate export induced by nutrient rich~~  
300 ~~Amazon outflow.~~

301 The most visible riverine  $Alk^*$  signals are in the Arctic due to the large riverine runoff  
302 into this comparatively small basin, ~~the intermediate to high  $A_T$  of high latitude river water (Cai~~  
303 ~~et al., 2008),~~ and the confinement of this low-density riverine water to the surface (Jones et al.,  
304 2008; Yamamoto-Kawai et al., 2008; Azetsu-Scott et al., 2010). Figure 4d shows the high Arctic  
305  $Alk^*$  plume is confined to the top  $\sim 200$  m. Figure 3 shows that these high  $Alk^*$  values extend  
306 along the coast of Greenland and through the Labrador Sea.  $Alk^*$  decreases with increasing  
307 salinity in this region (Fig. 6d) due to mixing between the fresh high  $Alk^*$  surface Arctic waters  
308 and the salty lower  $Alk^*$  waters of the surface Atlantic. Gascard et al. (2004a, b) suggest that  
309 high  $Alk^*$  waters along the coast of Norway are part of the Norwegian Coastal Current, and  
310 originate in the Baltic and North Seas where there are also strong riverine inputs (Thomas et al.,  
311 2005).

312 ~~Several mid-latitude rivers empty into marginal seas where PACIFICA, GLODAP, and~~  
313 ~~CARINA have no measurements, so we rely on data published in regional studies. Beldowski et~~  
314 ~~al. (2010) survey the carbonate system in the Baltic Sea and find distributions indicative of~~  
315 ~~mixing with outflow from several rivers. One of these, the Daugava, flows across a limestone~~  
316 ~~rich catchment and has an exceptionally high  $A_T$  of  $3172 \mu\text{mol kg}^{-1}$ . The Mississippi River also~~  
317 ~~has a very high  $A_T$  ( $2074 \mu\text{mol kg}^{-1}$ ) (Cai et al., 2008). Keul et al. (2010) report  $A_T$  and salinity~~

318 ~~distributions in waters offshore of the river mouth from which we calculate seawater  $Alk^*$  values~~  
319  ~~$>150 \mu\text{mol kg}^{-1}$ . We extrapolate a linear fit of  $Alk^*$  against salinity for data collected near the~~  
320 ~~river mouth to 0 salinity to estimate the Mississippi endmember outflow  $Alk^*$  as  $2201 \mu\text{mol kg}^{-1}$ .~~  
321 ~~The Changjiang (Yangtze) River also has an alkaline outflow estimated as  $1780 \mu\text{mol kg}^{-1}$  by~~  
322 ~~Cai et al., (2008) and  $2874\text{--}3665 \mu\text{mol kg}^{-1}$  by Chen et al., (2005). This river empties into the~~  
323 ~~Yellow Sea where Chou et al. (2009) reported data that we use to estimate an  $Alk^*$  of  $1978 \mu\text{mol}$~~   
324  ~~$\text{kg}^{-1}$  for the riverine end member (we assume nitrate concentrations of  $5 \mu\text{mol kg}^{-1}$ ).~~

325 Elevated  $Alk^*$  can also be seen in the Bay of Bengal with surface values  $\sim 100 \mu\text{mol kg}^{-1}$   
326 higher than those in the central Indian Ocean. This bay has two high  $A_T$  rivers that join and flow  
327 into it, the Brahmaputra ( $A_T = 1114 \mu\text{mol kg}^{-1}$ ) and the Ganges ( $A_T = 1966 \mu\text{mol kg}^{-1}$ ) (Cai et al.,  
328 2008). Figure 87 provides  $Alk^*$  depth sections for both areas. The riverine  $Alk^*$  plume can be  
329 clearly seen in the top 50 m of the Bay of Bengal. No similar increase is seen in the Arabian Sea  
330 where the Indus River ( $1681 \mu\text{mol kg}^{-1}$ ) discharges only  $\sim 1/10$ th of the combined volume of the  
331 Brahmaputra and the Ganges.

332 The Amazon River is the largest single riverine marine  $A_T$  source. This river has low  $A_T$   
333 ( $369 \mu\text{mol kg}^{-1}$  (Cai et al., 2008)), but has the largest water discharge volume of any river,  
334 exceeding the second largest—the Congo—by a factor of  $\sim 5$  (Dai and Trenberth, 2002).  
335 Consequently, the Amazon discharges approximately 50% more  $A_T$  per year than the river with  
336 the second largest  $A_T$  discharge, the Changjiang (Cai et al., 2008). The Amazon's influence can  
337 be seen as a region of abnormally low salinity and  $A_T$  in Fig. 2a and b. Despite the high  
338 discharge volume, the influence is only barely visible as a region of elevated  $Alk^*$  in Fig. 2c due  
339 to the comparatively low Amazon  $Alk^*$ . However, the influence of the Amazon on  $Alk^*$  can be  
340 seen in the seasonal  $Alk^*$  cycle in the Amazon plume. Figure 7 provides a map of  $Alk^*$  for this

341 region scaled to show the influence of this low  $Alk^*$  river in the Northern Hemisphere (a) winter  
 342 and (b) summer months. The higher  $Alk^*$  found for summer months is consistent with Amazon  
 343 discharge and  $A_T$  seasonality (Cooley et al., 2007) and Moore et al.'s (1986) radium isotope  
 344 based finding that Amazon River outflow comprises 20-34% of surface water in this region in  
 345 July compared to only 5-9% in December.

346

### 347 3.4 Regional inorganic carbonate cycling

348 The Red Sea portion of Fig. 8 is strongly depleted in  $Alk^*$ , and contains the lowest single  
 349  $Alk^*$  measurement in our dataset,  $-247 \mu\text{mol kg}^{-1}$ . The GEOSECS expedition Red Sea  
 350 alkalinity measurements are from the GEOSECS expedition (Craig and Turekian, 1980) predate  
 351 alkalinity reference materials (Dickson et al., 2007), but ~~the very low values~~ are supported by  
 352 more recent measurements (Silverman et al., 2007). ~~We~~ Like Jiang et al. (2014), we attribute low  
 353 Red Sea  $Alk^*$  to exceptionally active calcium carbonate ~~mineral~~ formation.

354 The Red Sea is one of the only regions where calcium carbonate saturation is sufficiently  
 355 high for inorganic carbonate precipitation to significantly contribute to overall carbonate  
 356 precipitation (Milliman et al. 1969; Silverman et al., 2007). Notably, saturation remains high at  
 357 depth in the Red Sea (see Section 4.2). Despite this, ~~calcium~~ carbonate sediments in the modern  
 358 Red Sea are mostly biogenic aragonitic corals and pteropod shells (Gevirtz and Friedman, 1966).  
 359 However, in this region, pores ~~left as shells dissolve due to~~ in sediments are filled in with high-  
 360 magnesium calcite cement (Almogi-Labin et al., 1986). We hypothesize biogenic carbonates are  
 361 dissolved by  $\text{CO}_2$  from sedimentary ~~buildup of carbon dioxide from~~ organic matter  
 362 remineralization ~~as occurs elsewhere (e.g. Hales and Emerson, 1997; Hales, 2003; Boudreau,  
 363 2013) are filled in with high-magnesium calcite cement (Almogi-Labin et al., 1986). The~~

364 ~~hypothesis), but~~ that ~~inorganic precipitation is an important sink for  $A_T$  in the high deep~~ Red Sea  
 365 ~~is consistent with the prevalence of biogenic~~ calcium carbonate ~~shells if saturation leads to~~  
 366 inorganic re-calcification ~~follows sedimentary dissolution of the biogenic carbonates in sediment~~  
 367 ~~pores.~~

368 Inorganic calcium carbonate has recently been found as metastable ikaite (a hydrated  
 369 calcium carbonate mineral with the formula  ~~$\text{CaCO}_3 \cdot 6\text{H}_2\text{O}$~~   $\text{CaCO}_3 \cdot 6\text{H}_2\text{O}$ ) in natural sea ice  
 370 (Dieckmann et al., 2008). Ikaite cycling provides a competing explanation for the high Arctic  
 371 surface  $Alk^*$  values if high  $A_T$  low-salinity ikaite-rich ice melt becomes separated from low  $A_T$   
 372 high-salinity rejected brines. However, riverine  $A_T$  inputs ~~are a better~~ explain the  
 373 magnitude of the feature: The  $\sim 5$  mg ikaite  $\text{L}^{-1}$  sea ice Dieckmann et al. (2008) found in the  
 374 Antarctic could only enrich  $A_T$  of the surface 100 m  ~~$A_T$~~  by  ~~$\sim 101$~~   $\mu\text{mol kg}^{-1}$  for each meter of ice  
 375 melted, and Arctic surface 100 m  $Alk^*$  is elevated by  $59 \mu\text{mol kg}^{-1}$  relative to the deeper Arctic  
 376 in our gridded dataset. By contrast, Jones et al. (2008) estimate a  $\sim 5\%$  average riverine end-  
 377 member contribution to the shallowest 100 m of this region, which accounts for  $\sim 55 \mu\text{mol kg}^{-1}$   
 378  $Alk^*$  enrichment. Also, surface  $Alk^*$  in the Southern Ocean—which has sea ice but lacks major  
 379 rivers—is not similarly elevated relative to phosphate (Fig. 2) or ~~relative to~~ deep  $Alk^*$  (Fig. 43).

380

#### 381 4. Controls on the calcite saturation state ~~of calcium carbonate~~

382 The  $Alk^*$  tracer provides an opportunity to estimate the impact of carbonate cycling on  
 383 the ~~carbonate mineral~~ calcite saturation, ~~and address the first part of the question we raised in the~~  
 384 Introduction. In addition to (1) carbonate cycling, ~~carbonate mineral~~ calcite saturation is affected  
 385 by ~~are~~ (2) organic matter cycling, (3) freshwater cycling, (4) ~~depth~~ pressure changes ~~of~~ on  
 386 seawater, (5) heating and cooling, and (6)  $A_T$  changes from nitrogen fixation and denitrification.

Field Code Changed

387 For each of these six processes, we estimate the standard deviation of the net influence of the  
 388 process globally by considering the standard deviation of a “reference” tracer  $R_i$  for the  
 389 process, “ $\sigma_{R_i}$ ”, where  $R_i$  is  $Alk^*$  for  $CaCO_3$  cycling, phosphate for organic matter  
 390 cycling, salinity for freshwater cycling, pressure for depth changes, temperature for  
 391 heating and cooling, and  $N^*$  (Gruber and Sarmiento, 1997) for nitrogen fixation and  
 392 denitrification. We use the standard deviation of the reference tracer as a measure of the oceanic  
 393 range of the net influence of the corresponding process. We measure the impact of this range on

394 carbonate mineral saturation using a metric  $M$ , which we define as:

$$395 \quad M_i = \sigma_{R_i} |S_{R_i}| \quad M_i = \sigma_{R_i} |S_{R_i}| \quad (6)$$

396 where  $S_{R_i}$  is the carbonate saturation sensitivity to a unit process change in  $R_i$ ,  
 397 which we estimate in Appendix A. We are interested in the relative importance  $I$  of our 6  
 398 processes, so we also calculate the percentage that each metric value estimate contributes to the  
 399 sum of all 6 metric value estimates:

$$400 \quad I_i = 100\% \times \frac{\sigma_{R_i} |S_{R_i}|}{\sum_{i=1}^6 \sigma_{R_i} |S_{R_i}|} \quad I_i = 100\% \times \frac{M_i}{\sum_{i=1}^6 M_i} \quad (7)$$

401 We derive and estimate our metric and its uncertainty in Appendix A. We carry out our analysis  
 402 for the full water column assuming it to be isolated from the atmosphere (section 4.1), and also  
 403 for just the top 50 m of the water column assuming it to be well-equilibrated with the atmosphere  
 404 (section 4.2). Finally, we consider how equilibration with an atmosphere with a changing  $pCO_2$   
 405 alters surface carbonate saturation.

406

407 *4.1 Process importance in atmospherically-isolated mean seawater from all ocean depths*

Field Code Changed

408 Our metric  $M_i$  is an estimate of the standard deviation of the  $\Omega_c$  global distribution  
 409 of  $\Omega_c$  resulting from the  $i$ th process. Our relative process importance metric  $I_i$  is an estimate  
 410 of the percentage of overall  $\Omega_c$  variability of the  $\Omega_c$  distribution variability that can be  
 411 attributed to that process. We provide  $M$  and  $I$  values for mean seawater from the full water  
 412 column alongside the  $X_R^i$ ,  $S_{X_R^i}$ , and  $\sigma_{X_R^i}$ ,  $R_i$ ,  $S_{R_i}$ , and  $\sigma_{R_i}$  values used to estimate them in Table 1.  
 413 These calculations assume that the seawater is isolated from the atmosphere.

414 Relative process importance estimates  $I$  indicate organic matter cycling (48%) is the  
 415 dominant process controlling carbonate calcite saturation for mean seawater. Changing pressure  
 416 (28%) is the second most important process, followed by calcium carbonate cycling (17%),  
 417 temperature changes (4%), nitrogen fixation and denitrification (1.21%), and freshwater cycling  
 418 (0.78%).

#### 420 4.2 Process importance in well-equilibrated surface seawater

421 ~~We~~In Table 2 we provide  $M_i$  values for well-equilibrated seawater in the top 50 m of  
 422 the ocean alongside the  $R_i$ ,  $R_i$ ,  $\sigma_{R_i}$ ,  $\sigma_{R_i}$ ,  $S_{R_i}$ ,  $S_{R_i}$  used to estimate them in Table 2. These surface  
 423 seawater  $M_i$  values are calculated assuming the water remains equilibrated with an  
 424 atmosphere with 400  $\mu\text{atm}$   $p\text{CO}_2$ . We test the validity of this assumption by also estimating  $M$   
 425 for the observed global  $p\text{CO}_2$  variability from incomplete equilibration. However, we do not  
 426 include this  $M$  value estimate in the denominator of Eq. (7) so  $I$  values for surface seawater are  
 427 calculated in the same way as in the Takahashi et al. (2009) global data product. This test reveals  
 428 transient air-sea disequilibria are indeed important for surface ocean calcite saturation, but only  
 429 as a secondary factor when considered globally. Despite this, it is important to recognize that

Field Code Changed

Formatted: Font: Italic

430 air-sea equilibration following a process is not instantaneous, and that the  $S_{R_i}$  value estimates in  
 431 section 4.1 will be better for estimating short term changes following fast acting processes such  
 432 as spring blooms (e.g. Tynan et al., 2014) or upwelling events (e.g. Feely et al., 1988). We omit  
 433 the disequilibrium  $M$  value estimate from the denominator of Eq. (7) to allow  $I$  values for surface  
 434 seawater to be compared to  $I$  values from mean seawater globally.

Field Code Changed

435 Warming and cooling are the dominant processes controlling  $\frac{\Omega_c}{\Omega_c}$  for well-  
 436 equilibrated surface seawater (76%). The large increase in  $\frac{M}{M}$  for warming and cooling  
 437 relative to the value calculated for mean seawater is due to lower equilibrium  $C_T$  at higher  
 438 temperatures. Freshwater cycling is the second most important process (13%), followed by  
 439 carbonate cycling (8%), organic matter cycling (2%), pressure changes (1%), and denitrification  
 440 and nitrogen fixation (0.4%). The increased importance of freshwater cycling is because  
 441 freshwater dilutes  $C_T$  by more than the equilibrium  $C_T$  decreases from  $A_T$  dilution, so carbon  
 442 uptake tends to follow freshwater precipitation and carbon outgassing follows evaporation.  
 443 Carbonate cycling is less important because  $A_T$  decreases with carbonate precipitation lead to  
 444 lower  $C_T$  at equilibrium. Organic matter cycling is much less important because atmospheric re-  
 445 equilibration mostly negates the large changes in  $C_T$ . Pressure ~~variability is less important~~  
 446 ~~simply changes are negligible~~ because we only consider water in the ~~top surface~~ 50 m. Our air-  
 447 sea disequilibrium  $M$  estimate suggests surface disequilibria are as comparably important to  
 448 freshwater cycling for surface calcite saturation ~~as freshwater cycling~~, but substantially less  
 449 important than temperature changes ~~-(this would correspond to an  $I$  value of ~14%).~~

Field Code Changed

Field Code Changed

450 The dominance of warming and cooling and freshwater cycling over carbonate cycling is  
 451 most evident in the Red Sea where high temperatures (>25 °C) and high salinities (>40 ~~g/kg~~)  
 452 lead to surface calcite saturations exceeding 6 despite extremely low  $Alk^*$  (<-200  $\mu\text{mol kg}^{-1}$ ).

453 The deep Red Sea is also unusual for having deep water that was warm ( $\leftrightarrow$  when it last left contact  
 454 with the atmosphere (the Red Sea is  $>20$  °C at  $>1000$  m depth), which-). This provides high  
 455 initial deep calcite saturation that—combined with decreased influence of pressure changes at  
 456 higher temperatures—keeps  $\Omega_c$  deep Red Sea  $\Omega_c > 3$ . Similarly, the lowest surface saturation  
 457 states are in the Arctic where there are low temperatures, low salinity, and high  $Alk^*$  from  
 458 riverine inputs. The importance of warming and cooling is also evident when considering the  
 459 broad similarities suggested by the correlation between the global surface calcite saturation and  
 460 the surface temperature ( $R^2 = 0.96$ ) shown for our gridded dataset in Fig. 9. The lowest surface  
 461 saturation states correspond to Arctic regions where both the temperature and the salinity are low  
 462 (see Fig. 2b); 8.

Field Code Changed

463

Formatted: Line spacing: Multiple 1.15 li

## 464 5. Conclusions

465  $Alk^*$  isolates the portion of the  $A_T$  signal that varies in response to calcium carbonate  
 466 cycling and the riverine and hydrothermal sources exchanges with terrestrial and sedimentary  
 467 environments from the portion that varies in response to freshwater and organic matter cycling.  
 468 The salinity normalization we use has the advantage over previous salinity normalizations that it  
 469 mixes allows our tracer to mix linearly and changes change in a 2:1 ratio with  $C_T$  in response to  
 470 carbonate cycling. We highlight the following insights from  $Alk^*$ :

471 (1) *Alk\* distribution:* The  $Alk^*$  distribution clearly shows the influence of biological  
 472 cycling including such features as the very low  $Alk^*$  in the Red Sea due to the high calcium  
 473 carbonate precipitation there. We also find evidence of strong riverine  $A_T$  sources near in the  
 474 mouths Bay of several major rivers Bengal and in the Arctic. A plot of  $Alk^*$  against salinity  
 475 reveals We show river inputs likely dominate over the large  $A_T$  input from small influences of

476 ~~ikaite cycling on the Amazon River. Arctic alkalinity distribution.~~

477 ~~(2) Impact of rivers on carbonate saturation: Rivers have high  $Alk^*$  compared to surface~~  
 478 ~~waters and might thus be expected to lead to high carbonate ion concentrations. However,~~  
 479 ~~because of the low salinity (and hence low  $A_T$  and calcium ion concentrations), mixing with~~  
 480 ~~seawater tends to decrease seawater  $\Omega_c$ . The sensitivities we calculate in Appendix A suggest~~  
 481 ~~that a 1:1 mixture between river water and surface seawater would have a lower  $\Omega_c$  than surface~~  
 482 ~~seawater unless the river water has an  $Alk^*$  exceeding  $\sim 2600 \mu\text{mol kg}^{-1}$ . This  $Alk^*$  is more than~~  
 483 ~~twice the mean riverine  $A_T$  of  $1100 \mu\text{mol kg}^{-1}$  of Cai et al. (2008). Mixtures of river water and~~  
 484 ~~seawater must thus be subjected to net evaporation, net warming, and/or air-sea  $p\text{CO}_2$~~   
 485 ~~disequilibrium before  $\Omega_c$  will be in line with typical surface seawater.~~

486 ~~(3) Influence of calcium carbonate cycling on marine calcium carbonate/calcite~~  
 487 ~~saturation:  $Alk^*$  allows us to quantify the net influence of calcium carbonate cycling on marine~~  
 488 ~~calcium carbonate/calcite saturation. ~~At the~~For well-equilibrated surface waters, carbonate~~  
 489 ~~cycling is less influential for calcite saturation than gas exchange driven by warming and~~  
 490 ~~cooling, air-sea disequilibrium, and freshwater cycling. At depth, the carbonate cycling signal is~~  
 491 ~~smaller than the signal from organic matter cycling ~~or~~ and from pressure changes. In general~~  
 492  ~~$Alk^*$  and carbonate saturation are inversely related to each other. For example, subtropical gyres~~  
 493 ~~have the highest surface saturation states despite having the lowest open-ocean  $Alk^*$  values.~~  
 494 ~~Here, high temperatures, strong net evaporation, and lower concentrations of recently upwelled~~  
 495 ~~remineralized  $C_T$  dominate over the low  $Alk^*$ . Similarly, in the deep ocean, saturation is the~~  
 496 ~~lowest where  $A_T$  and thus  $Alk^*$  are increasing from calcium carbonate dissolution. This is due to~~  
 497 ~~high pressures, low temperatures, and an abundance of remineralized carbon, as discussed by~~  
 498 ~~Broecker and Peng (1987). Temperature is the dominant control for surface carbonate on calcite~~

499 saturation ~~globally~~ of surface waters in equilibrium with the atmosphere. This accounts for the  
 500 low calcite saturation states in the cold surface of the Arctic and Southern Oceans; despite high  
 501 regional  $Alk^*$ , and high calcite saturations in the warm ~~deep Red Sea~~ subtropics despite low  
 502 regional  $Alk^*$ .

503 ~~The values in Table A3 allow us to compare the impact of the modern anthropogenic~~  
 504 ~~atmospheric  $pCO_2$  increase of  $\sim 120 \mu atm$  on  $CaCO_3$  saturation levels to the impact of other~~  
 505 ~~climate changes. The increase of  $\sim 120 \mu atm$  is 4.4 times as large as the modern surface ocean~~  
 506  ~~$pCO_2$  standard deviation of  $27 \mu atm$ . We calculate this decrease in global surface carbonate ion~~  
 507 ~~saturation levels is equivalent to the effect one would get from a  $\sim 7$  to  $8^\circ C$  cooling.~~

Formatted: Font color: Auto

508 ~~(4) Monitoring the impact of~~ intend to use  $Alk^*$  for two future projects. First,  $Alk^*$  is  
 509 superior to  $A_T$  for monitoring and modeling changes in marine chemistry resulting from changes  
 510 in carbonate cycling with ocean acidification ~~on carbonate biomineralization with  $Alk^*$~~ . We  
 511 ~~propose  $Alk^*$  as a model diagnostic that specifically targets calcium carbonate cycling and as a~~  
 512 ~~tracer to monitor the impact of ocean acidification on carbonate cycling. Regarding the latter,~~  
 513 ~~Ilyina et al. (2009) used models to estimate the biogenic carbonate precipitation response to~~  
 514 ~~ocean acidification, and to determine when corresponding  $A_T$  changes would become detectable~~  
 515 ~~by repeat hydrography. However,~~  $A_T$  varies substantially in response to freshwater cycling ~~that~~  
 516 ~~is also changing with climate.  $Alk^*$  is mostly insensitive to freshwater cycling, and thus, so  $Alk^*$~~   
 517 ~~trends would better distinguish carbonate cycling shifts from shifts in hydrology.~~

Formatted: Font: Not Italic

518 ~~For related future work, we aim to use the gridded global  $Alk^*$  distribution with~~ may be  
 519 able to be detected sooner and more confidently attributed to changes in calcium carbonate  
 520 cycling than trends in  $A_T$ . Preliminary explorations of Earth System Model output suggest time  
 521 of trend emergence for the alkalinity trends discussed by Ilyina et al. (2009) could be reduced by

Formatted: Font: Not Italic

522 as much as a factor of 5. Secondly, we will estimate global steady state  $Alk^*$  distributions using  
523  $Alk^*$  sources and sinks from varied biogeochemical ocean circulation models alongside  
524 independent water mixing and transport estimates (e.g. Khatiwala et al., 2005; 2007) ~~to infer the~~  
525 ~~magnitude of global sources and sinks of calcium carbonate.~~ We will interpret ~~these~~  
526 ~~estimates~~ findings in the context of ~~the riverine and hydrothermal sources and sinks of  $A_T$  in the~~  
527 ~~ocean, and investigate the degree to~~ two hypotheses proposed to explain evidence for calcium  
528 carbonate dissolution above the aragonite saturation horizon: (1) that organic matter  
529 remineralization creates undersaturated microenvironments that promote carbonate dissolution in  
530 portions of the water column which ~~carbonate cycling varies regionally with carbonate~~  
531 ~~saturation~~ are chemically supersaturated in bulk, and (2) that high-magnesium calcite and other  
532 impure minerals allow chemical dissolution above the saturation horizon.

533

#### 534 **Acknowledgements**

535 We thank Eun Young Kwon for contributions to early versions of this research. We also  
536 thank the US National Science Foundation for research support (ANT-1040957), as well as the  
537 numerous scientists and crew that contributed to the datasets used in this study. R. Key was  
538 supported by CICS grant NA08OAR432052. We also thank anonymous reviewers for their  
539 helpful and constructive comments.

540

#### 541 **References**

542 Almogi-Labin, A., B. Luz, and J. Duplessy (1986), Quaternary paleo-oceanography, pteropod  
543 preservation and stable-isotope record of the Red Sea, *Palaeogeogr., Palaeoclimatol.,*  
544 *Palaeoecol.*, 57, 195-211, DOI: 10.1016/0031-0182(86)90013-1.

- 545 Anderson, L. A. and J. L. Sarmiento (1994), Redfield ratios of remineralization determined by  
546 nutrient data analysis, *Global Biogeochem. Cycles*, 8, 65-80, doi: 10.1029/93GB03318.
- 547 Azetsu-Scott, K., A. Clarke, K. Falkner, J. Hamilton, E. P. Jones, C. Lee, B. Petrie, S.  
548 Prinsenberg, M. Starr, and P. Yeats (2010), Calcium carbonate saturation states in the waters  
549 of the Canadian Arctic Archipelago and the Labrador Sea, *J. Geophys. Res. Oceans*, 115,  
550 C11.
- 551 Beldowski, J., A. Löffler, B. Schneider, and L. Joensuu (2010), Distribution and biogeochemical  
552 control of total CO<sub>2</sub> and total alkalinity in the Baltic Sea, *J. Mar. Sys.*, 81, 252-259.
- 553 [Berelson, W. M., W. M. Balch, R. Najjar, R. A. Feely, C. Sabine, and K. Lee \(2007\), Relating](#)  
554 [estimates of CaCO<sub>3</sub> production, export, and dissolution in the water column to measurements](#)  
555 [of CaCO<sub>3</sub> rain into sediment traps and dissolution on the sea floor: A revised global](#)  
556 [carbonate budget, \*Global Biogeochem. Cycles\*, 21, GB1024, doi: 10.1029/2006GB002803.](#)
- 557 Boudreau, B. P. (2013), Carbonate dissolution rates at the deep ocean floor, *Geophys. Res. Lett.*,  
558 40, 1-5, doi: 10.1029/2012GL054231.
- 559 [Broecker, W. S., and T. H. Peng \(1987\), The role of CaCO<sub>3</sub> compensation in the glacial to](#)  
560 [interglacial atmospheric CO<sub>2</sub> change, \*Global Biogeochem. Cycles\*, 1, 15-29.](#)
- 561 [Brewer, P. G. and J. C. Goldman \(1976\), Alkalinity changes generated by phytoplankton growth,](#)  
562 [Limnol. Oceanogr., 21, 108-117.](#)
- 563 [Brewer, P. G., G. T. F. Wong, M. P. Bacon, D. W. Spencer \(1975\), An oceanic calcium](#)  
564 [problem? \*Earth and Planet. Sci. Lett.\*, 26 \(1\), 81-87, doi: 10.1016/0012-821X\(75\)90179-X.](#)

565 Cai, W.-J. X. Guo, C. A. Chen, M. Dai, L. Zhang, W. Zhai, S. E. Lohrenz, K. Yin, P. J. Harrison,  
 566 Y. Wang (2008), A comparative overview of weathering intensity and  $\text{HCO}_3^-$  flux in the  
 567 world's major rivers with emphasis on the Changjiang, Huanghe, Zhujiang (Pearl) and  
 568 Mississippi Rivers, *Continental Shelf Res.*, 28, 1538-1549

569 ~~Chen, J., F. Wang, M. Meybeck, D. He, X. Xia, and L. Zhang (2005), Spatial and temporal~~  
 570 ~~analysis of water chemistry records (1958—2000) in the Huanghe (Yellow River) basin,~~  
 571 ~~*Global Biogeochem. Cycles*, 19, GB3016, doi:10.1029/2004GB002325.~~

**Formatted:** Font color: Custom  
Color(RGB(34,34,34)), Pattern: Clear (White)

572 ~~Chou, W., G. Gong, D. D. Sheu, C. Hung, T. Tseng (2009), *J. Geophys. Res.*, Surface~~  
 573 ~~distribution of carbon chemistry parameters in the East China Sea in summer 2007, *J.*~~  
 574 ~~*Geophys. Res.*, 114, C07026 doi: 10.1029/2008JC005128.~~

**Formatted:** Font color: Custom  
Color(RGB(34,34,34)), Pattern: Clear (White)

575 Craig, H., and K.K. Turekian (1980), The GEOSECS program 1976-1979, *Earth Planet. Sci.*  
 576 *Lett.*, 49, 263-265, doi: 10.1016/j.bbr.2011.03.031.

577 Dai, A. and K. E. Trenberth (2002), Estimates of freshwater discharge from continents: latitudi-  
 578 nal and seasonal variations, *J. Hydrometeorology*, 3, 660-687.

579 Dickson, A.G. (1981), An exact definition of total alkalinity and a procedure for the estimation  
 580 of alkalinity and total inorganic carbon from titration data, *Deep Sea Res. A*, 28 (6), 609-623,  
 581 doi: 10.1016/0198-0149(81)90121-7.

582 Dieckmann, G.S., G. Nehrke, S. Papadimitriou, J. Göttlicher, R. Steininger, H. Kennedy, D.  
 583 Wolf-Gladrow, and D. N. Thomas (2008), Calcium carbonate as ikaite crystals in Antarctic  
 584 sea ice, *Geophys. Res. Lett.*, 35, LO8051, doi:10.1029/2008GL033540.

585 Dickson, A. G. and F. J. Millero (1987), A comparison of the equilibrium constants for the

- 586 dissociation of carbonic acid in seawater media, *Deep-Sea Res. A*, 34, 1733-1743.
- 587 Feely, R. A., C. L. Sabine, K. Lee, F. J. Millero, M. F. Lamb, D. Greeley, J. L. Bullister, R. M.  
588 Key, T. H. Peng, and A. Kozyr (2002), In situ calcium carbonate dissolution in the Pacific  
589 Ocean, *Global Biogeochem. Cycles*, 16, 1144, doi: 10.1029/2002GB001866.
- 590 [Feely, R. A., R.H. Byrne, J. G. Acker, P. R. Betzer, C. A. Chen, J. F. Gendron, and M. F. Lamb](#)  
591 [\(1988\), Winter-summer variations of calcite and aragonite saturation in the northeast](#)  
592 [Pacific. \*Mar. Chem.\* 25, 3, 227-241.](#)
- 593 Fofonof, N. P., and R. C. Millard (1983), Algorithms for computations of fundamental properties  
594 of seawater. UNESCO Technical Papers in Marine Science No. 44, 53 pp.
- 595 Gascard, J. C., G. Raisbeck, S. Sequeira, F. Yiou, and K. Mork (2004), Correction to 'The  
596 Norwegian Atlantic Current in the Lofoten basin inferred from hydrological and tracer  
597 data(I-129) and its interaction with the Norwegian Coastal Current'. *Geophys. Res.*  
598 *Lett.*, 31(8).
- 599 Gascard, J. C., G. Raisbeck, S. Sequeira, F. Yiou, and K. Mork (2004), Correction to  
600 2003GL01803, *Geophys. Res. Lett.*, 31, L08302, doi:10.1029/2004GL020006, 2004.
- 601 Gevirtz, J. L., and G. M. Friedman (1966), Deep-Sea carbonate sediments of the Red Sea and  
602 their implications on marine lithification, *J. Sed. Petrol.*, 36, 143-151.
- 603 Gruber, N., and J. L. Sarmiento (1997), Global patterns of marine nitrogen fixation and  
604 denitrification, *Global Biogeochemical Cycles*, 11(2), 235-266.
- 605 Hales, B. (2003), Respiration, dissolution, and the lysocline. *Paleoceanogr.*, 18(4), 1099.

- 606 Hales, B., and S. Emerson (1997), Calcite dissolution in sediments of the Ceara Rise: In situ  
 607 measurements of porewater O<sub>2</sub>, pH, and CO<sub>2</sub> (aq). *Geochim. Cosmochim. Acta*, 61(3), 501-  
 608 514.
- 609 Hernández-Ayon, J., A. Zirino, A. G. Dickson, T. Camiro-Vargas, and E. Valenzuela (2007),  
 610 Estimating the contribution of organic bases from microalgae to the titration alkalinity in  
 611 coastal seawaters, *Limnol. Oceanogr.: Methods*, 5, 225-232.
- 612 Honjo, S., S. J. Manganini, R. A. Krishfield, and R. Francois (2008), Particulate organic carbon  
 613 fluxes to the ocean interior and factors controlling the biological pump: A synthesis of global  
 614 sediment trap programs since 1983, *Prog. Oceanogr.*, 76(3), 217-285.
- 615 Ilyina, T. R. E. Zeebe, E. Maier-Reimer, and C. Heinze (2009), Early detection of ocean  
 616 acidification effects on marine calcification, *Global Biogeochem. Cycles*, 23, GB1008, doi:  
 617 10.1029/2008GB003278.
- 618 Jiang, Z. P., T. Tyrrell, D.J. Hydes, M. Dai, and S.E. Hartman (2014), Variability of alkalinity  
 619 and the alkalinity-salinity relationship in the tropical and subtropical surface ocean, *Global*  
 620 *Biogeochem. Cycles*, 28(7), 729-742, doi: 10.1002/2013GB004678.
- 621 Jones, E. P., L. G. Anderson, S. Jutterström, L. Mintrop, and J. H. Swift (2008), Pacific  
 622 freshwater, river water and sea ice meltwater across Arctic Ocean basins: Results from the  
 623 2005 Beringia Expedition, *J. Geophys. Res. Oceans*, 113(C8).
- 624 Kanamori, S. and H. Ikegami (1982), Calcium-alkalinity relationship in the North Pacific, *J.*  
 625 *Oceanogr.*, 38, 57-62.

**Formatted:** Font: Times New Roman, 12 pt,  
 Font color: Custom Color(RGB(34,34,34)),  
 Pattern: Clear (White)

**Formatted:** Font: Times New Roman, 12 pt,  
 Font color: Custom Color(RGB(34,34,34)),  
 Pattern: Clear (White)

626 Kaushal, S. S., G. E. Likens, R. M. Utz, M. L. Pace, M. Grese, and M. Yepsen (2013), Increased  
627 river alkalization in the Eastern U.S., *Envi. Sci. Tech.*, *47*, 10302-10311, doi:  
628 10.1021/es401046s.

629 ~~Keul, N., J. W. Morese, R. Wanninkhof, D. K. Gledhill, and T. S. Bianchi (2010), Carbonate~~  
630 ~~chemistry dynamics of surface waters in the northern Gulf of Mexico, *Aquat. Geochem.*, *16*,~~  
631 ~~337-351, DOI:10.1007/s10498-010-9091-2.~~

**Formatted:** Font color: Custom  
Color(GB(34,34,34)), Pattern: Clear (White)

632 Key, R. M., A. Kozyr, C. L. Sabine, K. Lee, R. Wanninkhof, J. L. Bullister, R. A. Feely, F. J.  
633 Millero, C. Mordy, and T. H. Peng (2004), A global ocean carbon climatology: Results from  
634 Global Data Analysis Project (GLODAP), *Global Biogeochem. Cycles*, *18*, GB4031, doi:  
635 10.1029/2004GB002247.

636 Key, R. M., T. Tanhua, A. Olsen, M. Hoppema, S. Jutterström, C. Schirnack, S. van Heuven, X.  
637 Lin, D. Wallace and L. Mintrop (2009), The CARINA data synthesis project: Introduction  
638 and overview, *Earth Sys. Sci. Data*, *2*(1), 579-624.

639 Khatiwala, S., M. Visbeck, and M. A. Cane, (2005), Accelerated simulation of passive tracers in  
640 ocean circulation models, *Ocean Modelling*, *9*(1), 51-69.

641 Khatiwala, S. (2007), A computational framework for simulation of biogeochemical tracers in  
642 the ocean, *Global Biogeochemical Cycles*, *21*(3), GB3001.

643 Milliman, J. D., D. A. Ross, and T. L. Ku (1969), Precipitation and lithification of deep-sea  
644 carbonates in the Red Sea, *J. Sed Res.*, *39*(2), 724-736.

**Formatted:** Font color: Custom  
Color(GB(34,34,34)), Pattern: Clear (White)

645 Moore, W. S. (2010), The effect of submarine groundwater discharge on the ocean. *Marine Sci.*,  
646 2, 59-88, doi: 10.1146/annurev-marine-120308-081019

- 647 | [Moore, W. S.](#), J. L. Sarmiento, and R. M. Key (1986), Tracing the Amazon component of surface  
648 | Atlantic water using  $^{228}\text{Ra}$ , salinity, and silica, *J. Geophys. Res.*, *91* (C2), 2574-2580.
- 649 | Robbins, P. E. (2001), Oceanic carbon transport carried by freshwater divergence: Are salinity  
650 | normalizations useful?. *J. Geophys. Res.*, *106*(C12), 30939-30.
- 651 | Sarmiento, J. L., J. Dunne, A. Gnanadesikan, R.M. Key, K. Matsumoto, R. Slater (2002), A new  
652 | estimate of the  $\text{CaCO}_3$  to organic carbon export ratio. *Global Biogeochem. Cy.*, *16*(4), 1107.
- 653 | Sarmiento, J. L., N. Gruber, M. A. Brzezinski, and J. P. Dunne (2004), High-latitude controls of  
654 | thermocline nutrients and low latitude biological productivity. *Nature*, *427*(6969), 56-60.
- 655 | Silverman, J. B. Lazar, and J. Erez (2007), Effect of aragonite saturation, temperature, and  
656 | nutrients on the community calcification rate of a coral reef, *J. Geophys. Res.*, *112*,  
657 | CO05004, DOI: 10.1029/2006JC003770.
- 658 | Suzuki, T., M. Ishii, M. Aoyama, J. R. Christian, K. Enyo, T. Kawano, R. M. Key, N. Kosugi, A.  
659 | Kozyr, L. A. Miller, A. Murata, T. Nakano, T. Ono, T. Saino, K. Sasaki, D. Sasano, Y.  
660 | Takatani, M. Wakita and C. Sabine (2013), PACIFICA Data Synthesis Project.  
661 | ORNL/CDIAC-159, NDP-092. Carbon Dioxide Information Analysis Center, Oak Ridge  
662 | National Laboratory, U.S. Department of Energy, Oak Ridge, Tennessee.  
663 | doi:10.3334/CDIAC/OTG.PACIFICA\_NDP092.
- 664 | Takahashi, T., S. C. Sutherland, R. Wanninkhof, C. Sweeney, R. A. Feely, D. W. Chipman, B.  
665 | Hales, G. Friederich, F. Chavez, C. Sabine, A. Watson, D. C. E. Bakker, U. Schuster, N.  
666 | Metzl, H. Yoshikawa-Inoue, M. Ishii, T. Midorikawa, Y. Nojiri, A. Körtzinger, T. Steinhoff,  
667 | M. Hoppema, J. Olafsson, T. S. Arnarson, B. Tilbrook, T. Johannessen, A. Olsen, R.

668 Bellerby, C. S. Wong, B. Delille, N. R. Bates, and J. W. deBarr, (2009), Climatological mean  
 669 and decadal change in surface ocean pCO<sub>2</sub>, and net sea–air CO<sub>2</sub> flux over the global  
 670 oceans, *Deep Sea Res. II*, 56(8), 554-577.

671 Thomas, H., Y. Bozec, H. J. De Baar, K. Elkalay, M. Frankignoulle, L. S. Schiettecatte, G.  
 672 Kattner, and A. V. Borges (2005), The carbon budget of the North Sea. *Biogeosci.*, 2(1), 87-  
 673 96.

674 Tynan, E., T. Tyrrell, and E. P. Achterberg (2014). Controls on the seasonal variability of  
 675 calcium carbonate saturation states in the Atlantic gateway to the Arctic Ocean. *Mar. Chem.*  
 676 158 (2014) 1-9. doi: 10.1016/j.marchem.2013.10.010

677 van Heuven, S., D. Pierrot, E. Lewis, and D. Wallace (2009), MATLAB Program developed for  
 678 CO<sub>2</sub> system calculations, *ORNL/CDIAC-105b, Carbon Dioxide Information Analysis Center,*  
 679 *Oak Ridge National Laboratory, US Department of Energy, Oak Ridge, Tennessee.*

680 Velo, A., F. F. Perez, P. Brown, T. Tanhua, U. Schuster, and R. M. Key (2009), CARINA  
 681 alkalinity data in the Atlantic Ocean, *Earth Syst. Sci. Data*, 1, 45-61, doi:10.5194/essd-1-45-  
 682 2009.

683 de Villiers, S. (1998), Excess dissolved calcium in the ocean: a hydrothermal hypothesis, *Earth*  
 684 *and Plan. Sci. Lett.*, 164(3-4), 624-641.

685 Wolery, T. J., and N. H. Sleep (1988), Interactions of geochemical cycles with the mantle. In:  
 686 Gregor, C. B., R. M. Garrels, F. T. Mackenzie, and J. B. Maynard (eds) *Chemical cycles in*  
 687 *the evolution of the earth.* Wiley, New York, 77-103.

688 Wolf-Gladrow, D. A., R. E. Zeebe, C. Klaas, A. Körtzinger, and A. G. Dickson (2007), Total

Formatted: Space Before: 0 pt, After: 0 pt

Formatted: Font color: Custom  
 Color(34,34,34), Pattern: Clear (White)

689 alkalinity: The explicit conservative expression and its application to biogeochemical  
690 processes. *Marine chemistry*, 106(1), 287-300.

691 **Appendix A: Definition of the process importance metric  $M_i$**

692 In simplest terms, our metric is the product of the calcite saturation sensitivity to a  
 693 process and the variability of the net influence of the process globally. The difficulty in this  
 694 calculation lies in quantifying the “net influence of a process.” We first show how we change  
 695 coordinates so we can use reference tracers as a proxy measurement for these net influences.

696 Our metric for  $\Omega_C$  variability resulting from the  $i$ th process is expressed as  $M_i$ :

$$697 \quad M_i = \sigma_{P_i} \left| \frac{\partial \Omega_C}{\partial P_i} \right| \quad (A1)$$

698 where  $P_i$  is an abstract variable representing the net process influence (that we will later factor

699 out), and  $\frac{\partial \Omega_C}{\partial P_i}$  is the calcite saturation sensitivity to the process. We expand  $\frac{\partial \Omega_C}{\partial P_i}$

700 using the chain rule to include a term for  $\Omega_C$  sensitivity to changes in the reference tracer  $R_i$

701  $R_i$  (see section 4) and a term  $\frac{\partial R_i}{\partial P_i}$  representing changes in  $R_i$  resulting from the  $i$ th process:

$$702 \quad M_i = \sigma_{P_i} \left| \frac{\partial \Omega_C}{R_i} \frac{\partial R_i}{\partial P_i} \right| \frac{\partial \Omega_C}{\partial P_i} = \frac{\partial \Omega_C}{\partial R_i} \frac{\partial R_i}{\partial P_i} \quad (A2)$$

703 In practice, we calculate  $\Omega_C$  as a function of  $j = 7$  properties: (1) pressure, (2)

704 temperature, (3) salinity, (4) phosphate, (5) silicate, (6)  $A_T$ , and (7)  $C_T$  for mean seawater and

705  $p\text{CO}_2$  for surface seawater, so we use the chain rule again to further expand the  $\frac{\partial \Omega_C}{\partial P_i}$  terms

706 as follows:

$$707 \quad M_i = \sigma_{P_i} \left| \sum_{j=1}^7 \frac{\partial \Omega_C}{\partial X_j} \frac{\partial X_{j,i}}{\partial R_i} \right| \frac{\partial \Omega_C}{\partial R_i} = \sum_{j=1}^7 \frac{\partial \Omega_C}{\partial X_j} \frac{\partial X_{j,i}}{\partial R_i} \quad (A3)$$

Field Code Changed

708 Here, the  $\frac{\partial X_{j,i}}{\partial R_i}$   $\frac{\partial X_{j,i}}{\partial R_i}$  are assumed terms (assumptions detailed shortly) that relate the effect of  
 709 the  $i$ th process on the  $j$ th property to the effect of the process on  $R_i$ , and the  $\frac{\partial \Omega}{\partial X_j}$   $\frac{\partial \Omega}{\partial X_j}$  terms  
 710 reflect calcite saturation sensitivity to changes in the  $j$  properties used to calculate it.

711 We ~~assum~~make assumptions regarding the  $\frac{\partial X_{j,i}}{\partial X_R}$   $\frac{\partial X_{j,i}}{\partial X_R}$  terms: we relate changes in  
 712 temperature from sinking or shoaling to changes in pressure using the potential temperature ( $\theta$ )  
 713 routines of Fofonoff and Millard (1983); we assume freshwater cycling linearly concentrates  $A_T$ ,  
 714  $C_T$ , phosphate, and silicate by the same ratio that it changes salinity; we relate  $C_T$ , phosphate, and  
 715  $A_T$  changes from organic matter formation to changes in phosphate using the remineralization  
 716 ratios found by Anderson and Sarmiento (1994) and the empirical relationship of Kanamori and  
 717 Ikegami (1982); we also use Kanamori and Ikegami (1982)'s constant to relate changes in  $A_T$   
 718 from nitrogen fixation and denitrification to changes in  $N^*$  from these processes; and we assume  
 719 that an increase in  $A_T$  from calcium carbonate dissolution equals the  $Alk^*$  increase, and that the  
 720 corresponding increase in  $C_T$  equals half of this  $Alk^*$  increase. We neglect any changes in  $C_T$   
 721 from denitrification and nitrogen fixation because these changes are better thought of as organic  
 722 matter cycling occurring alongside nitrogen cycling.

723 We estimate  $\frac{\partial \Omega}{\partial X_j}$   $\frac{\partial \Omega}{\partial X_j}$  property sensitivity terms as the differences between  $\Omega_C$   $\Omega_C$   
 724 calculated before and after augmenting  $j$ th property by 1 unit.  $\Omega_C$   $\Omega_C$  is calculated with the  
 725 MATLAB CO2SYS routines written by van Heuven et al. (2009) using ~~with~~ the carbonate  
 726 system equilibrium constants of Mehrbach et al. (1973), as refit by Dickson and Millero (1987).  
 727 Seawater  $pCO_2$  is used in place of  $C_T$  for the surface seawater calculations (when  $j = 7$ ) to

Field Code Changed

728 calculate the change in  $\Omega_c$  that remains after the surface seawater is allowed to equilibrate  
729 with the atmosphere.

730 We assume that the distributions of our  $R_i$  reference properties are linearly related to  
731 the  $P_i$  net activities of their associated processes. This assumption implies:

$$732 \quad \sigma_P = \sigma_{R_i} \left| \frac{\partial P_i}{\partial R_i} \right| \quad \sigma_P = \sigma_{R_i} \left| \frac{\partial P_i}{\partial R_i} \right| \quad (A4)$$

733 We can then ~~combine Eqs.~~ substitute Eq. (A3) into Eq. (A2), and substitute this combined  
734 equation for  $\frac{\partial \Omega_c}{\partial P_i}$  and (A4) into Eq. (A1). We then and cancel the  $\frac{\partial P_i}{\partial R_i}$  and  $\frac{\partial R_i}{\partial P_i}$  terms to obtain:

$$735 \quad M_i = \sigma_{R_i} \left| \sum_{j=1}^7 \frac{\partial \Omega_c}{\partial X_j} \frac{\partial X_{j,i}}{\partial R_i} \right| = \sigma_{R_i} |S_{R_i}| \quad M_i = \sigma_{R_i} \left| \sum_{j=1}^7 \frac{\partial \Omega_c}{\partial X_j} \frac{\partial X_{j,i}}{\partial R_i} \right|$$

736 Here  $S_{R_i}$  equals the sum of the terms within the absolute value brackets and represents the  
737 ~~value~~ We then define our saturation sensitivity  $S_{R_i}$  as:

$$738 \quad S_{R_i} = \left| \sum_{j=1}^7 \frac{\partial \Omega_c}{\partial X_j} \frac{\partial X_{j,i}}{\partial R_i} \right| \quad (A6)$$

739 where  $S_{R_i}$  is the saturation sensitivity to a change in the  $i$ th process scaled to a unit change in the  
740 reference variable for that process. We can then substitute Eq. (A6) into Eq. (A5) to obtain Eq.

741 6. We use Eqn. (A6) to define  $S_{R_i}$  and Eqn. 6 to calculate  $M_i$ . We provide the  $\frac{\partial \Omega_c}{\partial X_j}$  and  $\frac{\partial X_{j,i}}{\partial R_i}$

742  $\frac{\partial \Omega_c}{\partial X_j}$  and  $\frac{\partial X_{j,i}}{\partial R_i}$  values we use to estimate  $S_{R_i}$  for atmospherically isolated seawater from all

743 depths in Table A1 and for well-equilibrated surface seawater in Table A3. We perform a

Field Code Changed

Formatted: Indent: First line: 0", Space After: 10 pt, Line spacing: Multiple 1.15 li, Widow/Orphan control

Field Code Changed

744 [sample  \$I\$  and  \$M\$  calculation in Supplementary Materials document SE.](#)

745 We use a Monte Carlo analysis to estimate variability and uncertainty in our metric  $M$   
 746 and our percent relative process importance  $I$  calculations. We calculate the standard deviations,  
 747  ~~$\sigma_M$~~  and  ~~$\sigma_I$~~   ~~$\sigma_M$~~  and  ~~$\sigma_I$~~ , of pools of 1000  $M$  and  $I$  estimates calculated after adjusting the  
 748 seawater properties  $X_i$  with a normally-distributed perturbation with a standard deviation equal to

749 the property standard deviation from the gridded dataset. We find  $\frac{\sigma_I}{I} \frac{\sigma_I}{I}$  is typically much

750 smaller than  $\frac{\sigma_M}{M} \frac{\sigma_M}{M}$ . This is because [carbonatecalcite](#) saturation sensitivity is typically

751 proportional to the [carbonatecalcite](#) saturation itself, so individual Monte Carlo  $M$  estimates vary  
 752 with the initial [carbonatecalcite](#) saturation and one another. Our  ~~$\sigma_M$~~   ~~$\sigma_M$~~  estimates are therefore

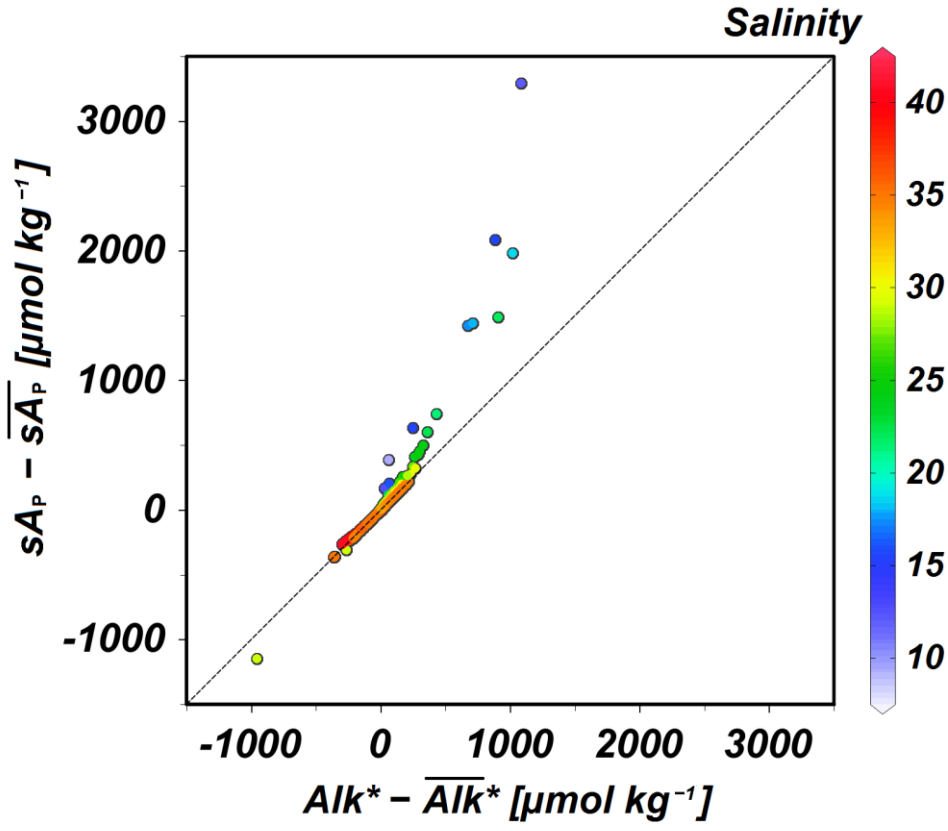
753 better thought of as measures of the ranges of sensitivities found in the modern ocean, while  ~~$\sigma_I$~~   
 754  ~~$\sigma_I$~~  represent variability in the relative importance of processes. We provide  ~~$\sigma_M$~~   ~~$\sigma_M$~~  and  ~~$\sigma_I$~~   ~~$\sigma_I$~~

755 for atmospherically isolated seawater globally in Table A2, and for well-equilibrated surface  
 756 seawater in Table A4.

757

758

Field Code Changed



Formatted: Line spacing: single, Widow/Orphan control, Position: Horizontal: Left, Relative to: Margin, Vertical: 0", Relative to: Paragraph, Horizontal: 0.13", Wrap Around

Formatted Table

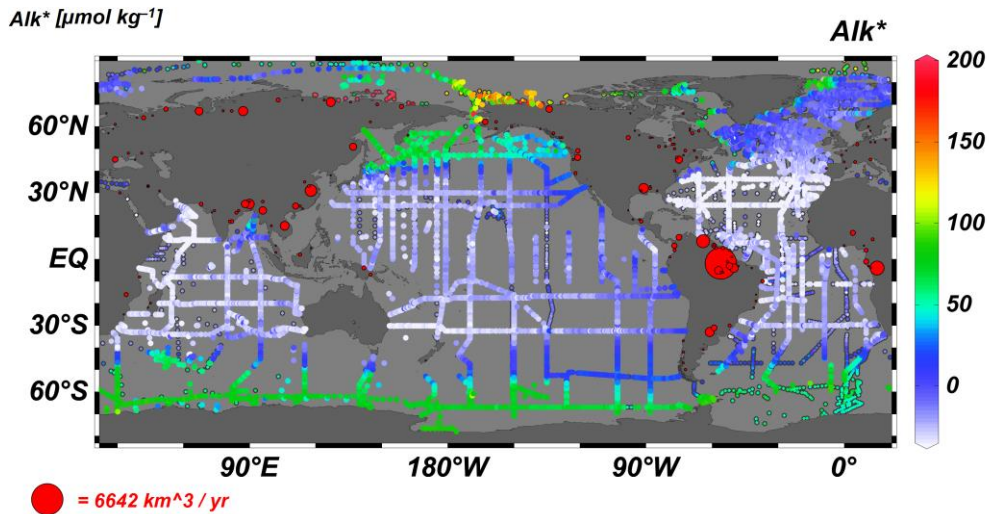


**Figure 1.** A map of station locations at which we use measurements to estimate  $Alk^*$  (in  $\mu\text{mol kg}^{-1}$ ). Dot color indicates surface  $Alk^*$ . Points with black borders indicate that either  $A_T$  was measured prior to 1992 (i.e. before reference materials were commonly used) or that no nitrate value was reported (in which case a nitrate concentration of  $5 \mu\text{mol kg}^{-1}$  is assumed). **Figure 1.** Mean-subtracted traditionally normalized potential alkalinity,  $sA_T$ , plotted against mean subtracted  $Alk^*$  for all data in our merged CARINA, PACIFICA, and GLODAP bottle data product. Salinity is indicated by dot color. The vast majority of data fall near the dashed 1:1 line which we provide for reference. However, the large deviations from this line, dominantly in low salinity Arctic data, demonstrate the non-linearity of the traditional salinity normalization  $sA_T$ . Red dots on land indicate the mouth locations and mean annual discharge volumes (indicated by dot size) of 200 large rivers, as given by Dai and Trenberth (2002).

**Formatted:** Widow/Orphan control, Position: Horizontal: Left, Relative to: Margin, Vertical: 0", Relative to: Paragraph, Horizontal: 0.13", Wrap Around

759

760

761

762

763

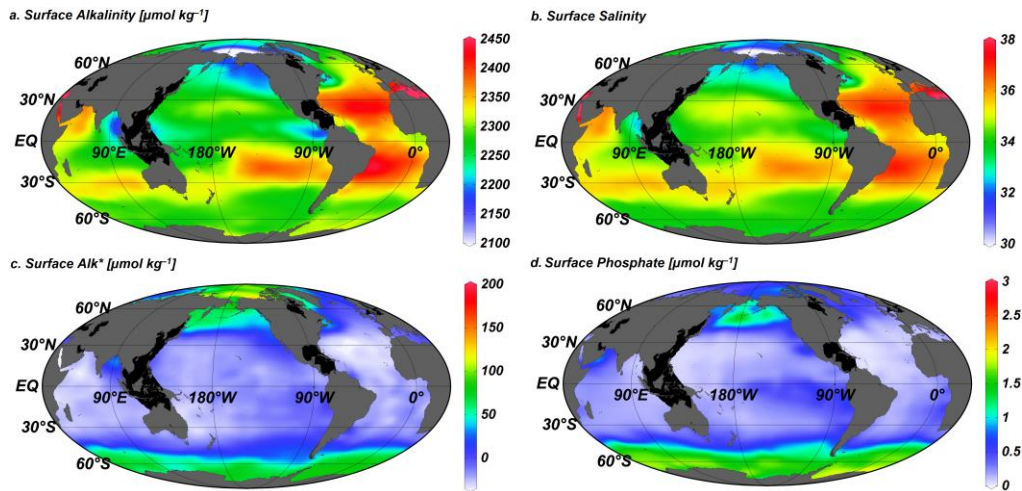


**Figure 2.** Global (a) total alkalinity  $A_T$ , (b) salinity, (c)  $\text{Alk}^*$ , and (d) phosphate distributions at the surface (10 m depth surface) from our gridded CARINA, PACIFICA, and GLODAP bottle data product. Areas with exceptionally poor coverage in the data used to produce the gridded product are blacked out.

764

765

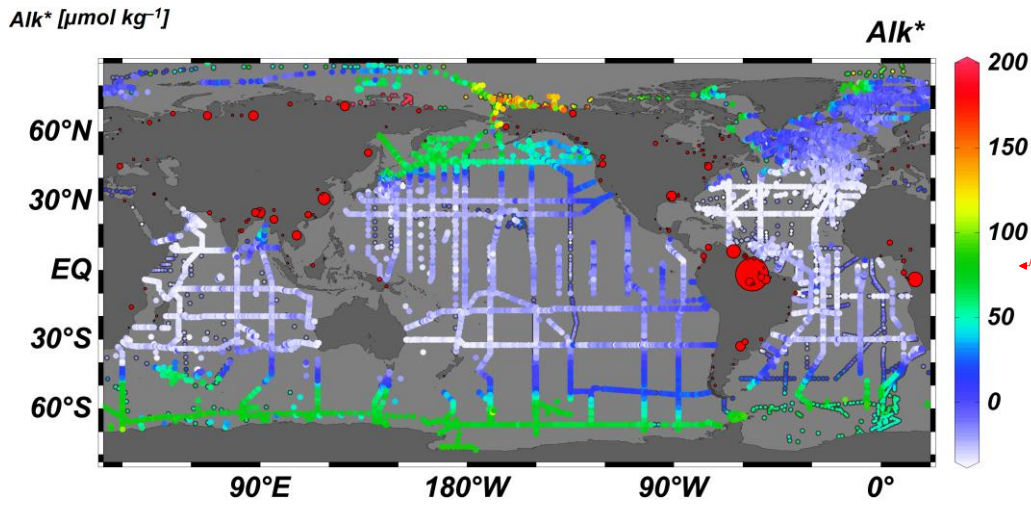
766

767

768

769

770



**Formatted:** Position: Horizontal: Left, Relative to: Column, Vertical: In line, Relative to: Margin, Horizontal: 0", Wrap Around

**Formatted Table**

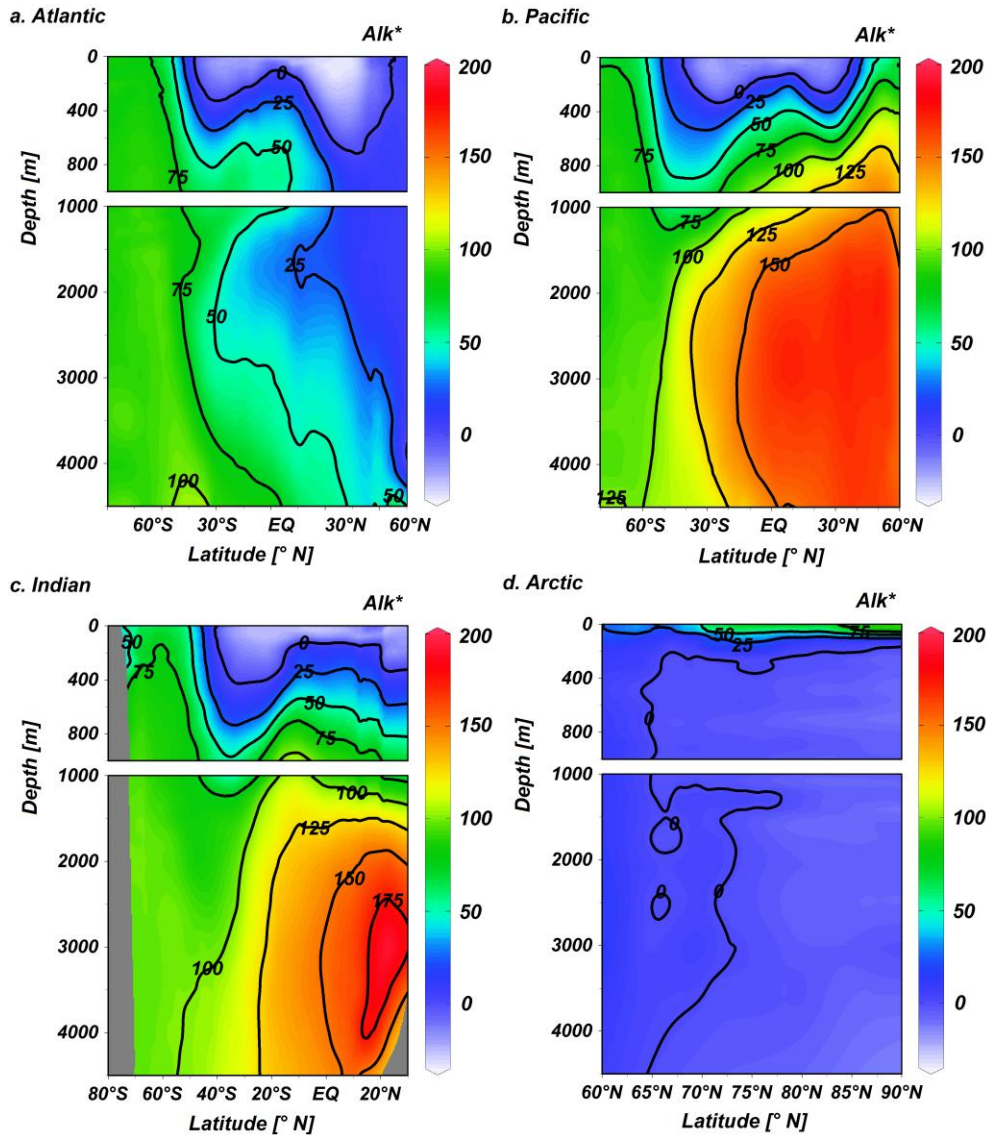


**Figure 3.**  $Alk^*$  values (in  $\mu\text{mol kg}^{-1}$ ) in top 50 m of the ocean plotted in color. **Figure 3.** Zonal mean gridded  $Alk^*$  (in  $\mu\text{mol kg}^{-1}$ ) in the (a) Atlantic, (b) Pacific, (c) Indian, and (d) the Arctic oceans plotted against latitude and depth. Points with black borders indicate that either  $A_T$  was measured prior to 1992 (i.e. before reference materials were commonly used) or that no nitrate value was reported (in which case a nitrate concentration of  $5 \mu\text{mol kg}^{-1}$  is assumed). Red dots on land indicate the locations and mean annual discharge volumes (indicated by dot size) of 200 of the world's largest rivers by volume and drainage area, as given by Dai and Trenberth (2002).

Formatted: Position: Horizontal: Left, Relative to: Column, Vertical: In line, Relative to: Margin, Horizontal: 0", Wrap Around

771

772

773

774

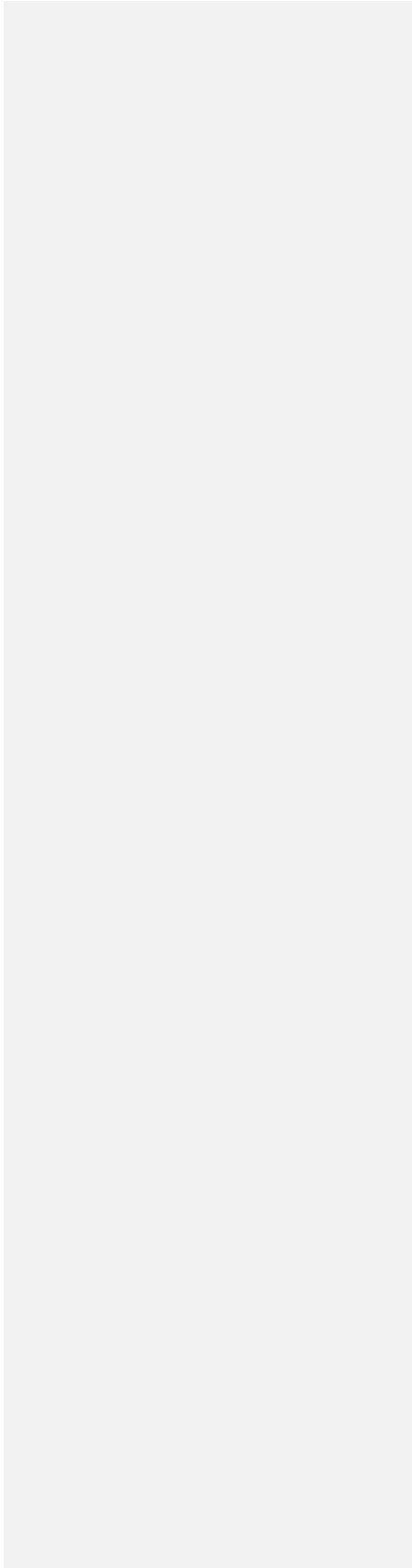
775

776

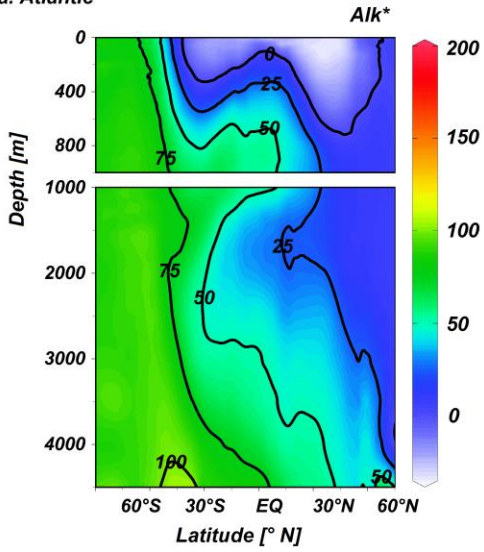
777

778

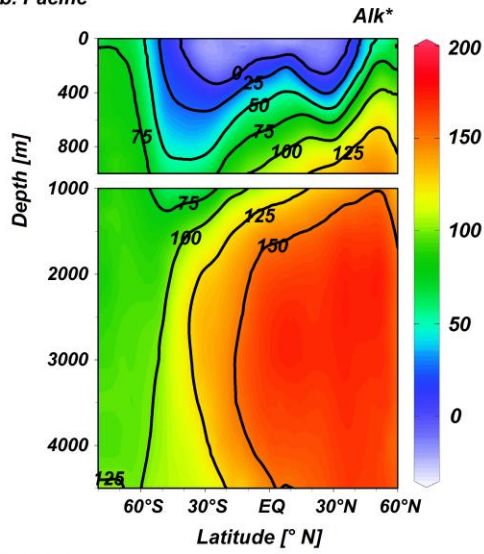
779



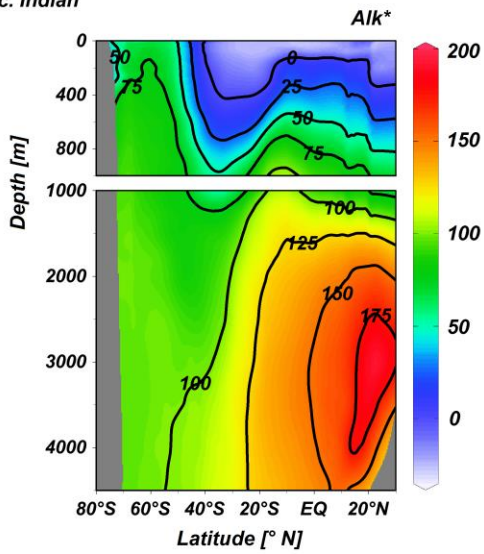
a. Atlantic



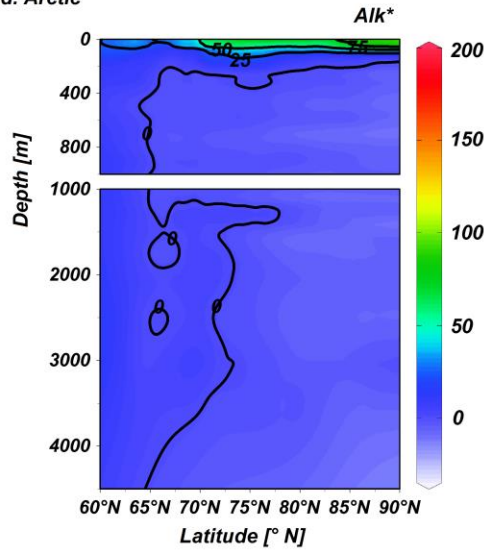
b. Pacific



c. Indian



d. Arctic



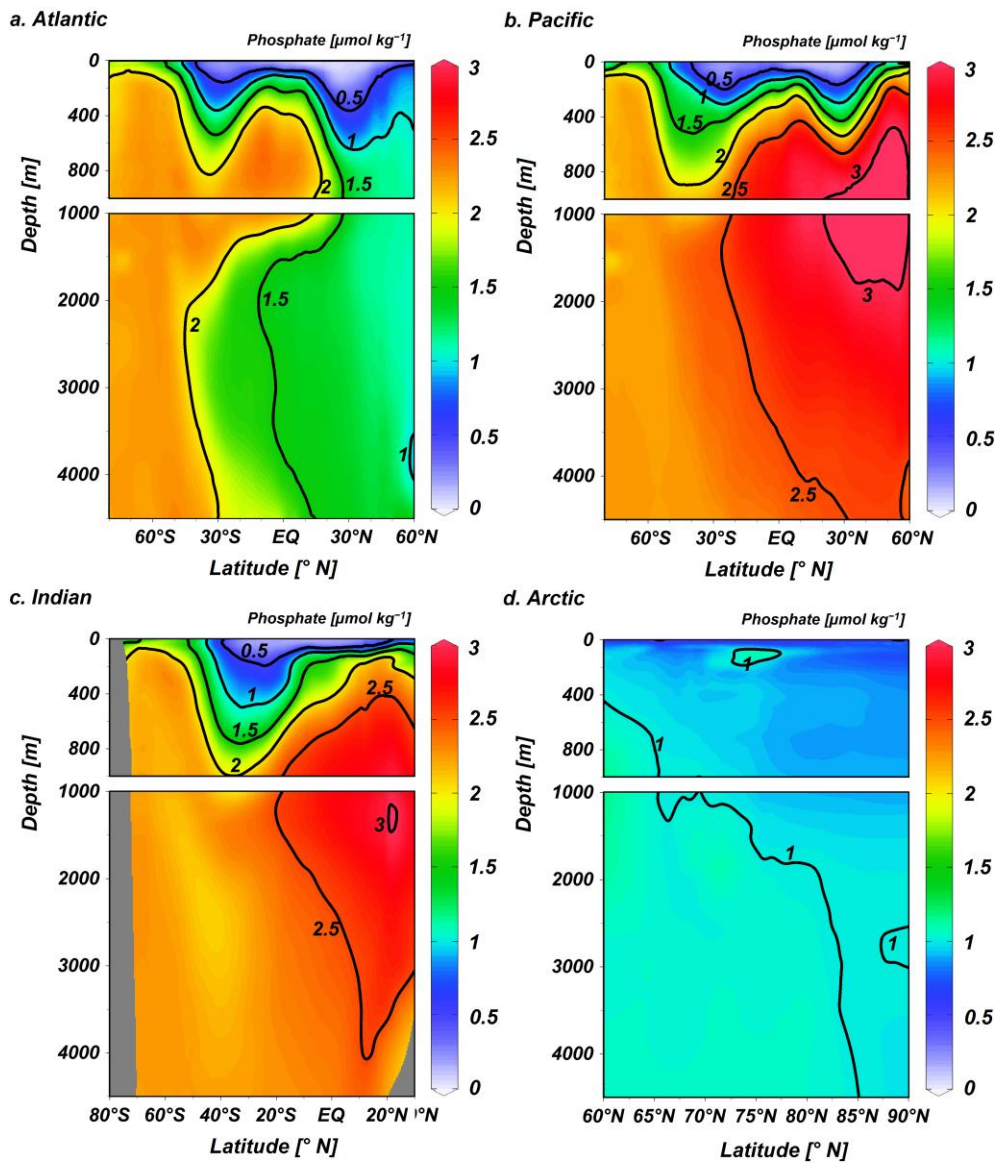


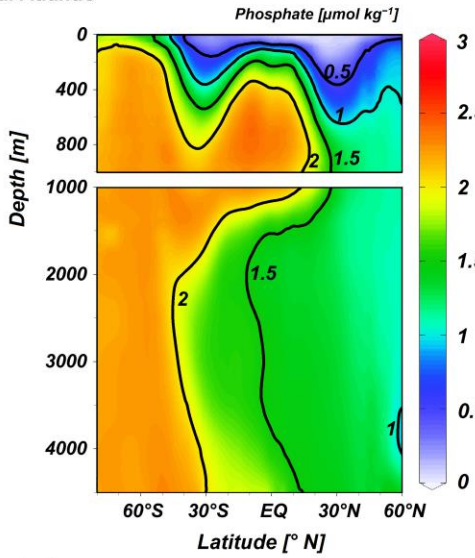
**Figure 4.** Zonal mean ~~ALL\* distributions~~gridded phosphate (in  $\mu\text{mol kg}^{-1}$ ) in the (a) Atlantic, (b) Pacific, (c) Indian, and (d) the Arctic oceans plotted against latitude and depth.

780

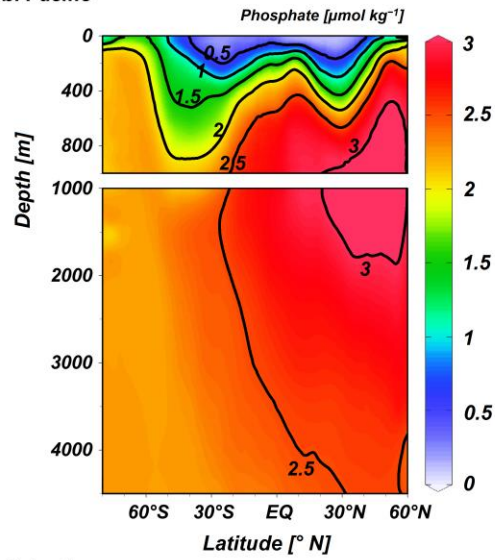
781

782

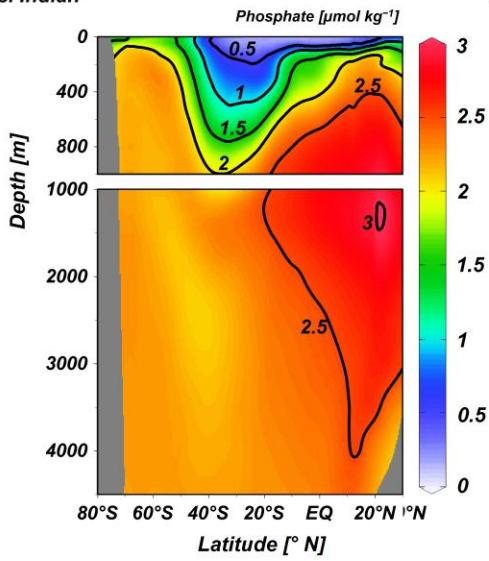
a. Atlantic



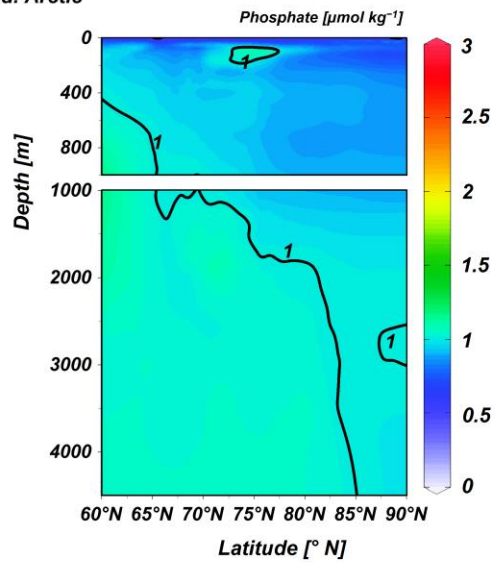
b. Pacific



c. Indian



d. Arctic



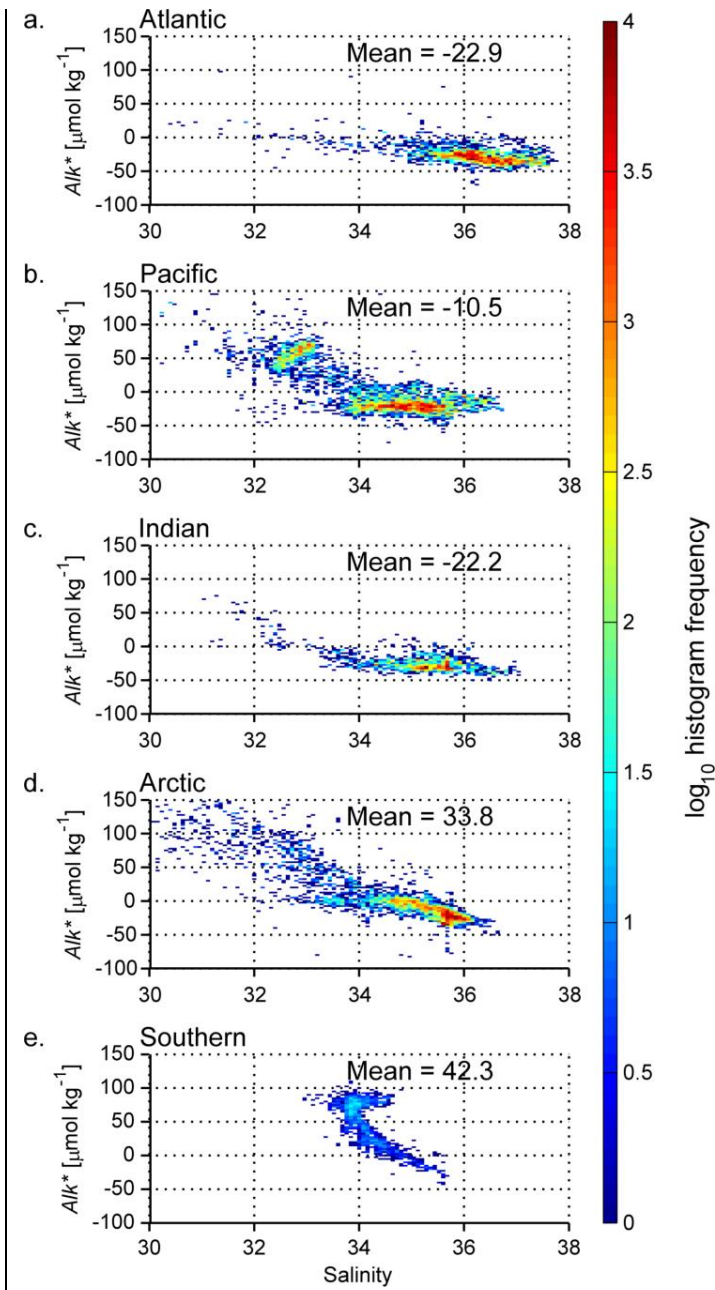


**Figure 5.** Zonal mean phosphate distributions (in  $\mu\text{mol kg}^{-1}$ ) in the (a) Atlantic, (b) Pacific, (c) Indian, and (d) the Arctic oceans plotted against latitude and depth. **Figure 5.** 2-D histograms indicating the log (base 10) of the number of measurements that fall within bins of Alk\* vs.

salinity with color. Data are limited to the top 50 m of the (a) Atlantic, (b) Pacific, (c) Indian, (d) Arctic, and (e) Southern Oceans. Where basins connect, the boundary between the Atlantic and the Arctic oceans is 40°N, between the Atlantic and the Indian is 20° E, between the Indian and the Pacific is 131° E, between the Pacific and the Atlantic is 70° W, and between the Southern Ocean and the other oceans is 40°S.

783

784

785

786

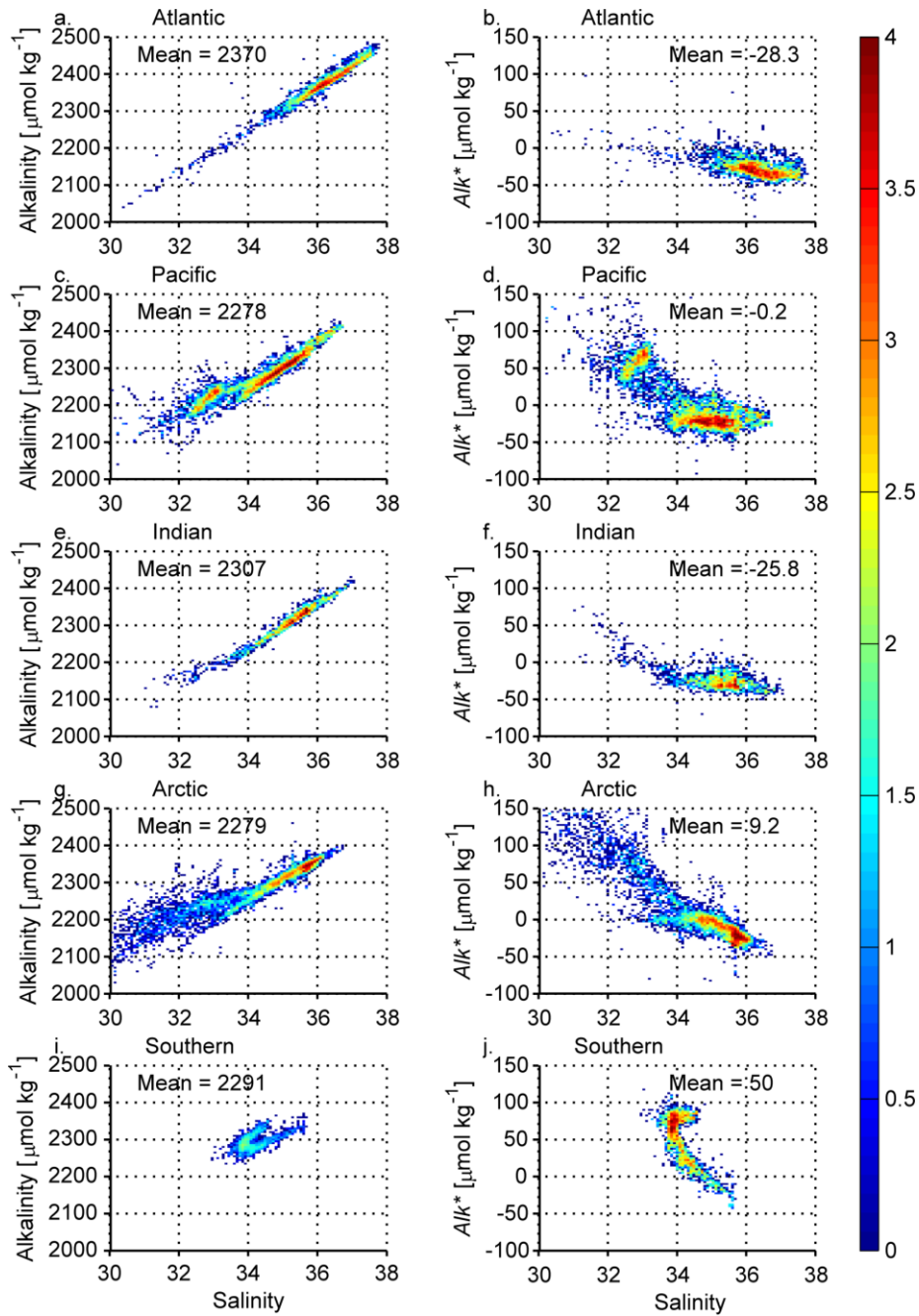


**Figure 6.** 2-D histograms indicating the log (base 10) of the number of measurements that fall within bins of  $A_T$  (a, c, e, g, i) and  $\text{Alk}^*$  (b, d, f, h, j) vs. salinity with color. Data are limited to

the top 50 m of the (a, b) Atlantic, (c, d) Pacific, (e, f) Indian, (g, h) Arctic, and (i, j) Southern Oceans. Due to the log scale, the vast majority of the measurements are found in the warmer colored bins. Where basins connect, the boundary between the Atlantic and the Arctic oceans is  $40^{\circ}\text{N}$ , between the Atlantic and the Indian is  $20^{\circ}\text{E}$ , between the Indian and the Pacific is  $131^{\circ}\text{E}$ , between the Pacific and the Atlantic is  $70^{\circ}\text{W}$ , and between the Southern Ocean and the other oceans is  $40^{\circ}\text{S}$ .

788

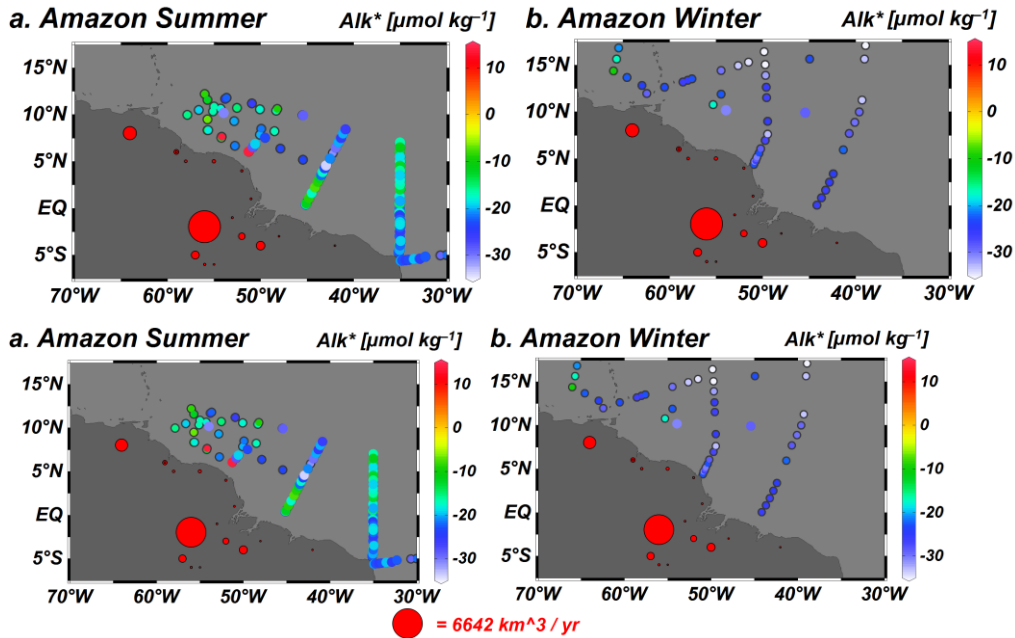


**Figure 76.**  $Alk^*$  (in  $\mu\text{mol kg}^{-1}$ ) in top 50 m of the ocean near the Amazon River outflow plotted in color, though with a narrower color scale than is used for all other plots. Panel (a) is limited to data collected in November through January, and in panel (b) is limited to measurements from May through July. The higher  $Alk^*$  values in Northern Hemisphere summer months are consistent with observations of higher quantities of Amazon derived water during these months (Moore et al., 1986). Points with black borders indicate that either the  $A_T$  was measured prior to 1992 (before reference materials were commonly used) or that no nitrate value was reported (in which case a nitrate concentration of  $5 \mu\text{mol kg}^{-1}$  is assumed). Red dots on land indicate the mouth locations and mean annual discharge volumes (indicated by dot size) of large rivers, as given by Dai and Trenberth (2002).

789

790

791

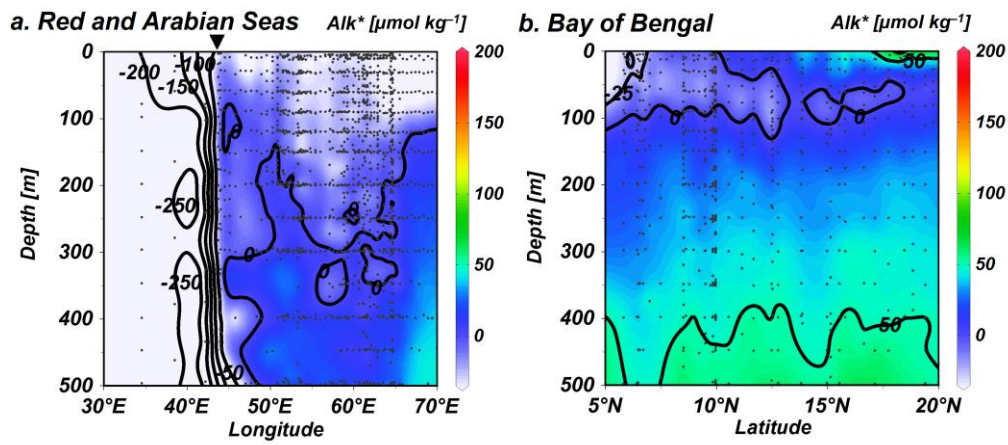
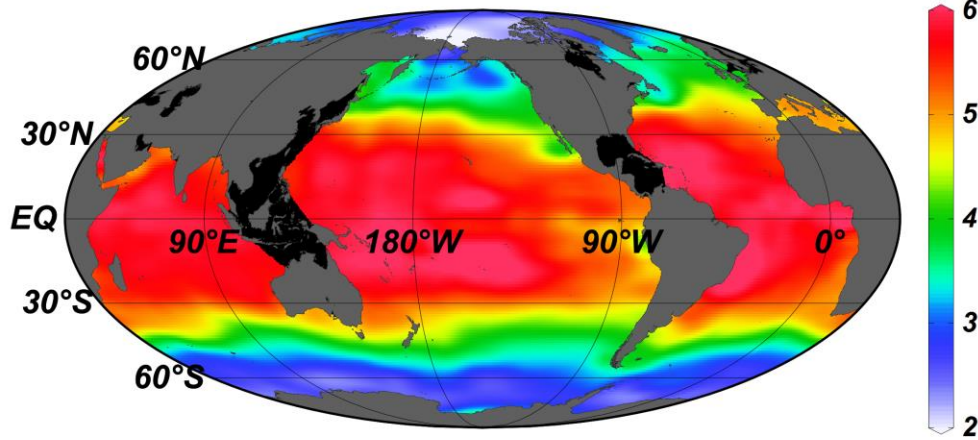


**Figure 87.**  $Alk^*$  distributions (in  $\mu\text{mol kg}^{-1}$ ) (a) between 5° and 30°N in the Red and Arabian Seas shown against longitude, and (b) between 75° and 100° E in the Bay of Bengal plotted against latitude. Small black dots indicate where data is present. The inverted triangle above (a) indicates the longitude of the mouth of the Red Sea.

792

793

a. Surface Calcite Saturation



b. Surface Temperature [ $^{\circ}\text{C}$ ]

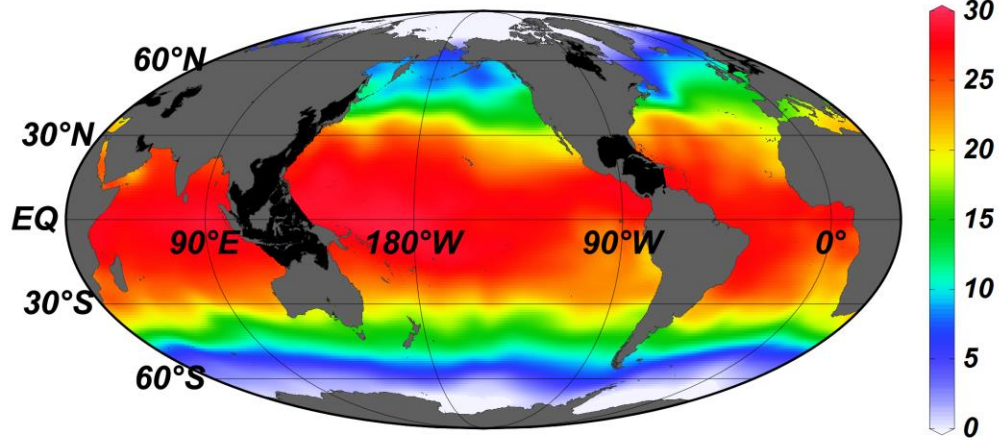


**Figure 98.** Gridded global (a)- calcite saturation, and (b) temperature at the surface (10 m depth surface) of our gridded CARINA, PACIFICA, and GLODAP bottle data product. —Areas with exceptionally poor coverage in the data used to produce the gridded product are blacked out.

795

**Table 1.** Metric estimates  $M_i$ , relative process importance percentages  $I_i$ , calcite saturation sensitivities  $S_{R_i}$ , and reference property standard deviations  $\sigma_{R_i}$  for the  $i = 6$  processes in atmospherically isolated mean seawater. These terms are estimated and  $M_i$  and  $I_i$  uncertainties in Appendix A.

**Process**

796

797

798

799

**Table 1.** Metric estimates  $M_i$ , relative process importance percentages  $I_i$ , calcite saturation sensitivities  $S_{R_i}$  to unit changes in the  $R_i$  reference properties, and reference property standard deviations  $\sigma_{R_i}$  for the  $i = 6$  processes in atmospherically isolated mean seawater from all ocean depths. See Appendix A for details on how these terms are estimated and explanation of how  $M_i$  and  $I_i$  uncertainties are obtained.

<u>Process</u>	<u><math>i</math></u>	<u><math>R_i</math></u>	<u><math>-S_{R_i}</math></u>	<u><math>\sigma_{R_i}</math></u>	<u><math>M_i</math></u>	<u><math>I_i</math></u>
Carbonate cycling	1	$Alk^*$	0.0043	53.5 $\mu\text{mol/kg}$	0.23	17%
Org. matter cycling	2	Phosphate	-0.0069	0.60 $\mu\text{mol/kg}$	0.66	48%
Freshwater cycling	3	Salinity	0.032	0.27	0.011	0.78%
Sinking / shoaling	4	Pressure	-0.00028	1411 db	0.4	28%
Warming / cooling	5	Temp.	0.014	4.20 $^{\circ}\text{C}$	0.06	4%
Denit./nit. fix.	6	$N^*$	-0.010	1.6 $\mu\text{mol/kg}$	0.017	1.2%

800

801

Formatted: Normal

Formatted Table

Formatted: Font: Not Italic

Deleted Cells

Deleted Cells

Deleted Cells

Deleted Cells

Deleted Cells

Deleted Cells

**Table 2.** Metric estimates  $M_i$ , relative process importance percentages  $I_i$ , calcite saturation sensitivities  $S_{R_i}$  to unit changes in the  $R_i$  reference properties, and reference property standard deviations  $\sigma_{R_i}$  for the  $i = 6$  processes in well-equilibrated surface seawater. ~~We provide~~ See Appendix A for details on how these terms are estimated and  ~~$M_i$  explanation of how  $M_i$  and  $I_i$  uncertainties in Appendix A are obtained.~~

Process	$i$	$R_i$	$S_{R_i}$	$\sigma_{R_i}$	$M_i$	$I_i$
Carbonate cycling	1	Alk*	0.0034	36.9 $\mu\text{mol/kg}$	0.13	7.8%
Org. matter cycling	2	Phosphate	-0.0045	0.51 $\mu\text{mol/kg}$	0.037	2.3%
Freshwater cycling	3	Salinity	0.20	0.86	0.22	13.2%
Sinking / shoaling	4	Pressure	-0.00083	15 db	0.011	0.70%
Warming / cooling	5	Temp.	0.14	8.8 $^{\circ}\text{C}$	1.2	76%
Denit. / nit. fix.	6	N*	-0.0043	1.5 $\mu\text{mol/kg}$	0.006	0.40%
$p\text{CO}_2$ disequilibria	$\dagger$	$p\text{CO}_2$	-0.0086	27 $\mu\text{atm}^*$	0.23	$\dagger$

\* standard deviation of the Takahashi et al. (2009) revised global monthly  $p\text{CO}_2$  climatology

$\dagger$  the  $M$  value for disequilibria is only calculated to test our assumption of surface seawater air-sea equilibration, and is omitted from calculations of  $I_i$  for comparison with Table 1.

Field Code Changed

804

805

**Table A1.**  $\frac{\partial \Omega_c}{\partial X_j}$   $\frac{\partial \Omega_c}{\partial X_j}$  (bold text) and  $\frac{\partial X_{j,i}}{\partial R_i}$   $\frac{\partial X_{j,i}}{\partial R_i}$  (italic text) terms used in Eq. (A5) for atmospherically isolated mean seawater from all ocean depths. These terms are specific to the  $j = 7$  (columns) properties we use to calculate  $\Omega_c$  and  $i = 6$  (rows) processes we consider.  $\Omega_c$  and  $i = 6$  (rows) processes we consider. Units for  $\frac{\partial \Omega_c}{\partial X_j}$  are the inverse of the listed  $X_j$  units. Units for  $\frac{\partial X_{j,i}}{\partial R_i}$  are the  $X_j$  units divided by the  $R_i$  units given in Table 1.

Properties $X_j$ units	Pressure db	Temp °C	Salinity	Phos. μmol/kg	Silicate μmol/kg	$A_T$ μmol/kg	$C_T$ μmol/kg	
$j$	1	2	3	4	5	6	7	
Mean seawater values	2235	3.7	34.71	2.15	49.0	2362	2254	
Process	$i$	<b>-0.00028</b>	<b>0.014</b>	<b>-0.011</b>	<b>-0.0085</b>	<b>-0.00012</b>	<b>0.0082</b>	<b>-0.0079</b>
Carbonate cycling	1	-	-	-	-	1	0.5	
Org. matter cycling	2	-	-	1	-	-20.16	117	
Freshwater cycling	3	-	1	0.062	1.4	68	65	
Sinking / shoaling	4	1	0.00010	-	-	-	-	
Warming / cooling	5	-	1	-	-	-	-	
Denit. / nit. fix.	6	-	-	-	-	-1.26	-	

806

807

Field Code Changed

808

809

**Table A2.** Monte Carlo derived estimates for  $M_i$  variability ( $\sigma_{M_i}$ ) and  $I_i$  variability ( $\sigma_{I_i}$ ) for atmospherically-isolated mean seawater from all ocean depths.

Process	$i$	$\sigma_{M_i}$	$\sigma_{I_i}$
Carbonate cycling	1	0.09	1%
Org. matter cycling	2	0.2	3%
Freshwater cycling	3	0.006	0.08%
Sinking / shoaling	4	0.2	5%
Warming / cooling	5	0.02	2%
Denit. / nit. fix.	6	0.006	0.1%

810

Field Code Changed

811

812

**Table A3.**  $\frac{\partial \Omega_c}{\partial X_j}$   $\frac{\partial \Omega_c}{\partial X_j}$  (bold text) and  $\frac{\partial X_{j,i}}{\partial R_i}$   $\frac{\partial X_{j,i}}{\partial R_i}$  (italic text) terms used in Eq. (A5) for well-equilibrated surface seawater. These terms are specific to the  $j = 7$  (columns) properties we use to calculate  $\Omega_c$  and  $i = 6$  (rows) processes we consider.  $\Omega_c$  and  $i = 6$  (rows) processes we consider. Units for  $\frac{\partial \Omega_c}{\partial X_j}$  are the inverse of the listed  $X_j$  units. Units for  $\frac{\partial X_{j,i}}{\partial R_i}$  are the  $X_j$  units divided by the  $R_i$  units given in Table 2.

Properties	Pressure	Temp	Salinity	Phos.	Silicate	$A_T$	$p\text{CO}_2$	
units	db	°C		$\mu\text{mol/kg}$	$\mu\text{mol/kg}$	$\mu\text{mol/kg}$	$\mu\text{atm}$	
$j$	1	2	3	4	5	6	7	
Mean seawater values	25	18.3	34.82	0.51	2.5	2305	350	
Process	$i$	<b>-0.00084</b>	<b>0.14</b>	<b>-0.022</b>	<b>-0.0038</b>	<b>-0.00013</b>	<b>0.0034</b>	<b>-0.0086</b>
Carbonate cycling	1	-	-	-	-	1	-	
Org. matter cycling	2	-	-	-	1	-20.16	-	
Freshwater cycling	3	-	1	0.015	0.072	65.9	-	
Sinking / shoaling	4	1	0.00010	-	-	-	-	
Warming / cooling	5	-	1	-	-	-	-	
Denit./nit. fix.	6	-	-	-	-	-1.26	-	

813

Field Code Changed

814

**Table A4.** Monte Carlo derived estimates for  $M_i$  variability ( $\sigma_{M_i}$ ) and  $I_i$  variability ( $\sigma_{I_i}$ ) for well-equilibrated surface seawater.

Process	$i$	$\sigma_{M_i}$	$\sigma_{I_i}$
Carbonate cycling	1	0.03	0.8%
Org. matter cycling	2	0.01	0.2%
Freshwater cycling	3	0.04	0.5%
Sinking / shoaling	4	0.001	0.03%
Warming / cooling	5	0.2	1%
Denit. / nit. fix	6	0.002	0.04%
$p\text{CO}_2$ disequilibria	†	0.05	†

† disequilibria are included only as a test of our assumption of surface seawater air-sea equilibration, so these  $M_i$  values are omitted from calculations of  $I$

Field Code Changed

815

816

817